UNIVERSITY OF GOTHENBURG
SCHOOL OF BUSINESS, ECONOMICS AND LAW

GARCH and GAS: Comparison of volatility models for Bitcoin in different exchanges

Department of Finance

Master's Thesis in Finance

Author:

Mohammad Rashidi Ranjbar

Advisor:

Dr. Marcin Zamojski

June 2020

Abstract

Different characteristics of cryptocurrencies have been investigated by a number of studies. In this study, I focus on conditional volatility of Bitcoin in three exchanges which are Coinbase, Bitfinex and Bitstamp. I investigate in-sample and out-of-sample performance of GARCH, GAS, Realized GARCH, GJR and EGARCH, and assess existence of inverse leverage effect. Moreover, multivariate GAS model with equi-correlation and constant correlation structures is applied. I find that, in the time period of this study, inverse leverage effect does not exist, and Normal GARCH-GAS model performs relatively better for out of sample forecasts. Furthermore, in multivariate part, I show that constant correlation t-GAS out performs other models with respect to AIC and BIC, and that estimated correlations, which are very close to one, provide evidence that while arbitrage opportunities exist across different markets, investors cannot diversify by investing in different markets.

Keywords: Bitcoin; Volatility Modelling; GAS; GARCH; Realized GARCH; Coinbase; Bitfinex; Bitstamp

Acknowledgement

Firstly, I would like to express my sincere gratitude to my advisor Marcin Zamojski for providing me with continuous and valuable helps, inputs and comments. In addition, I would like to express my gratitude to all my teachers at both University of Gothenburg and University of Tor Vergata for all their endeavors. Last but not least, I would like to thank my family: my parents and my grandparents who have supported me through all the steps of my life. Without help and support of you all, this would not be possible to achieve. I will always be grateful for all the helps and supports.

Contents

List of Tables

Figures

1. Introduction

Conditional variances or volatilities of asset returns are typically used to measure financial, and are in turn used in asset pricing, asset management, and risk management. Assets that have high volatility are considered riskier, and investors expect such assets to generate higher returns to compensate for the risk. Modelling of conditional variances of assets is one of important research areas in finance and is the focus of this study.

In this study, I evaluate price volatility for Bitcoin which was first introduced as a byproduct of another innovation, and has gained popularity and attention among not only traders but also researchers. Bitcoin and other cryptocurrencies are now traded by more than 50 million active market participants (Makarov & Antoinette, 2020). Moreover, development of Bitcoin derivative market provides evidence for importance of investigating volatility of Bitcoin. This study intends to evaluate in sample and out-of-sample performances of different volatility models when applied to Bitcoin prices in different exchanges and to investigate leverage effect for volatility.

For univariate study, I utilize GARCH(1,1), GAS(1,1), and Realized GARCH models, and compare how they perform for heavy tail distribution. In addition, GJR-GARCH, EGARCH and Realized GARCH with leverage function are included to assess asymmetric response. While stock markets have higher volatility after negative return, but (Baur & Dimpfl, 2018) find evidence of inverse effect for cryptocurrencies.

Furthermore, I utilize multivariate GAS , capable of absorbing outliers and observations from tails, with constant correlation and equi-correlation structures for multivariate analysis. While (Makarov & Antoinette, 2020) show existence of arbitrage opportunities across different exchanges, I estimate correlations which can be used to investigate diversification benefit. Except for EGARCH, which is included only with Normal distribution, for all the other models I include Normal and Student's t distribution densities.

For the empirical study, I consider three different exchanges: Coinbase, Bitstamp and Bitfinex. The sample period is August 10th 2016 to January 7th 2019, which includes a dramatic price rise during 2017. In this period, Coinbase was the biggest retail exchange, and Bitfinex is believed to be behind many of price manipulations in the time interval (Griffin & Shams, 2019).

Following estimation of different models, I compare their in-sample performances based on AIC and BIC information criteria. In-sample performance of GARCH and GAS models are comparable. The t-GAS shows lowest AIC and BIC and best in-sample performance compared to other models in its class. Among GJR and EGARCH models, GJR with Student's t distribution has the best in sample performance in all the markets. In addition, Realized GARCH with leverage and Student's t distribution exhibits best in-sample performance among models including a realized measure.

In addition, using Diebold-Mariano test statistic (Diebold & Mariano, 1995) and Mean Squared Prediction Error, I investigate out-of-sample performance of univariate models in the last 50 days of my period of study with an extending window design. I find that Normal GARCH (equivalent to Normal GAS) outperforms other models. However, this result can be due to the period considered for out of sample forecasts.

Estimation results of multivariate models show that constant correlation model with Student's t distribution has best in-sample performance. In addition, correlations are estimated approximately equal to one, providing evidence that markets are highly correlated. Furthermore, high correlation shows that although arbitrage opportunities may exist across markets, investing in Bitcoin in different markets does not provide a diversification benefit. Moreover, results of estimating univariate and multivariate models suggest possibility of factor structure, not only because of high correlation but also because of similar volatility forecasts.

In addition, all the univariate and multivariate models with Student's t distribution exhibit low degrees of freedom and heavy tail distribution. Moreover, forecasts of realized GARCH model with leverage depicts higher predictions for Coinbase than those for other markets. In addition, I find that the number of degrees of freedom estimated for Coinbase is lower than that of other markets, an observation that can serve as an explanation for higher predicted volatility of Coinbase.

The rest of this paper is structured as follows. Section 2 includes Literature Review which is given in four parts: Block chain, Market structure and efficiency, Univariate Volatility and Multivariate Volatility. Section 3 provides Methodology used in this study and is decomposed to three subsections: Univariate, Multivariate and Model Selection. Section 4 gives a detailed description of data set used in this study, and section 5 presents results of empirical study. In section 6, I perform a brief simulation study, and in section 7, I present conclusion.

2. Literature Review

2.1 Block chain

First introduced as a byproduct of another innovation, Bitcoin has gained popularity and attention among not only traders but also researchers. Bitcoin and other cryptocurrencies are now traded by more than 50 million active market participants (Makarov & Antoinette, 2020). Although the intriguing idea of digital currency existed for long time, Bitcoin---the first cryptocurrency---was created in late 2008 by unknown person or group of people under the pseudonym of "Satsohi Nakamoto" (Ølnes, 2016).

There are several issues in creating digital currency. One worth mentioning is double spending. Bitcoin prohibits repeated spending of the same unit of currency and ensures transfer of money from the paying account. Indeed, the blockchain technology provides necessary basis on which some cryptocurrencies, such as Bitcoin, Ethereum, Litecoin and Ripple, are established and overcome the problem of double spending (Crosby, et al., 2016).

Blockchain technology has other important characteristics such as alleged anonymous spending, i.e., inability to recognize the entity who spends the bitcoin (Nakamoto & Bitcoin, 2008). However, several previous studies show methods by which transactions can be traced (Meiklejohn, et al., 2013) and (Ron & Adi, 2013). Nevertheless, researchers provide new privacy patterns and cryptocurrencies, independent from Bitcoin, in response to methods of tracking transactions, but many of configurations proposed by them suffer from either inefficiency or insecurity (Heilman, et al., 2016).

Blockchain technology facilitates transactions in a decentralized manner. This means that there is no centralized entity to keep records (Bouri, et al., 2016) and utilizes peer to peer system for transferring data among nodes. In fact, market information is stored in nodes which need to solve complex mathematical problems to facilitate transactions (Crosby, et al., 2016). Nodes check the information with each to ensure consistency.

On one hand, solving mathematical problems and remaining connected to network requires consumption of energy. On another hand, blockchain system must ensure zero benefit for miners (nodes) and for possible attackers (Budish, 2018). Therefore, miners are rewarded with Bitcoin for providing liquidity, and blockchain network is designed such that attacks become expensive.

(Ølnes, 2016) suggests that blockchain has shown the potential to be utilized for smart governments: one of the usages could be validating documents in the public sector.

2.2 Market structure and efficiency

Cryptocurrency exchanges differ structurally from other markets. For example, exchanges are open continuously. Data from cryptocurrency markets can be observed at high frequency and without interruption, while stock markets are open during weekdays and facilitate trades in specific time intervals.

In contrast to fiat currency that central banks can print without limitations, total supply of Bitcoin that will ever be produced is capped (Brandvold, et al., 2015). This is a design choice as for other cryptocurrencies the total supply is not limited. Furthermore, while value of Bitcoin is determined with respect to supply and demand, there are other cryptocurrencies which derive their value with respect to other indicators, such as Tether which is supposedly pegged to US dollar. Despite many in online communities and press being suspicious of this claim, exchanges facilitate trades with Tether as well (Griffin & Shams, 2019).

Market structure and efficiency of cryptocurrencies have been investigated by a number of previous studies. (Urquhart, 2016) shows that although Bitcoin market is inefficient over sample period of this study, it moves toward efficiency in late subsample period, gradually evolving to an efficient market. (Makarov & Antoinette, 2020) illustrate that cross-venue arbitrage opportunities exist across different Bitcoin exchanges. They also show that the arbitrage opportunities are present for weeks, and are larger across countries or regions. Long memory in Bitcoin return time series between 2011 and 2017 is tested by (Bariviera, et al., 2017) concluding that market became more stable in latter period.

Properties of Bitcoin as a specific asset class have been researched by different studies. (Selgin, 2015) argues that Bitcoin can be considered speculative commodity, and (Bouri, et al., 2016) evaluate Bitcoin for diversification and hedging, concluding that it can be only used as hedge against dramatic down movements in Asian stocks.

An illiquid market without a central authority may face difficulties to handle large trading volumes, causing jumps in price (Scaillet, et al., 2017). Utilizing unique opportunity created by data leak of

Mt. Gox, (Scaillet, et al., 2017) evaluate jumps in Bitcoin market, finding presence of approximately one jump day per week in the time period of their study.

Fluctuations in price of Bitcoin have been the focus of different studies. (Griffin & Shams, 2019) show that Tether has been used to manipulate price of Bitcoin during its unprecedented dramatic price increase in 2017. (Brandvold, et al., 2015) argue that although in western world people previously trusted central banks, following Euro crisis this attitude has changed, and posit that dissimilar prices in different exchanges are due to providing cheaper withdrawing and depositing.

2.3 Univariate Volatility

In this study, I investigate volatility of Bitcoin in different exchanges, so the volatility literature is divided into univariate and multivariate sections. I present literature review of volatility modelling and its application to Bitcoin and Cryptocurrencies. Volatility modelling has received much attention in financial literature, as it is a paramount factor in asset pricing.

Parametric volatility modelling is classified into two different classes: observation-driven and parameter-driven models. Basic stochastic volatility model, developed by (Taylor, 1982) , contains an unobserved variance component, modeled by an autoregressive process, in the form of exponential (for details see (Shephard, 2005)). The class of observation-driven models includes the famous Generalized Auto Regressive Conditional Heteroskedastic (GARCH) model of (Engle, 1982) and (Bollerslev, 1986). In addition, realized measures are gaining popularity and attention as a third alternative (Andersen, et al., 1999).

There are many different specifications of GARCH models. The most notable include, GJR-GARCH model of (Glosten, et al., 1993), which considers asymmetric effects of returns in GARCH(1,1) model by including additional coefficient for negative shocks, and EGARCH of (Nelson, 1991) which does not need parameter restrictions and considers volatility as a multiplicative function of past innovations.

In the class of observation-driven models, we have also Generalized Autoregressive Score (GAS) model of (Creal, et al., 2013) which encompasses many other observation-driven models including the aforementioned GARCH models. GAS can be utilized to arrive at new formulations for volatility in a structured way and leverages all information in the likelihood function. Moreover, it has also been shown by (Blasques, et al., 2015) that updates used in GAS models are optimal.

Volatility of cryptocurrencies has been assessed by a number of recent research studies. For instance, (Katsiampa, 2017) applies combination of autoregressive and different GARCH-based models to find the optimal one with the highest goodness-of-fit for Bitcoin. He finds that AR-CGARCH performs better than other models considered with respect to information criterion measures. However, I will show in Chapter 4 that for the period of current study, there is no need to perform autoregressive model. (Baur & Dimpfl, 2018) analyze volatility effect of positive and negative returns on volatility of 20 cryptocurrencies. They find that cryptocurrency markets are more volatile after a positive shock. This finding is in stark contrast to stock markets. They attribute the finding to ‘fear of missing out’ referring to noise trading of uniformed investors after positive shocks.

Classic GARCH models are susceptible to an important shortcoming. While the markets might be extremely volatile during the day, low frequency, for example daily sampling, can lead to misleading measures for volatility. (Andersen & Bollerslev, 1998) discuss application of high-frequency intra-daily data sets to forecast volatility. High-frequency realized volatility is shown to be potentially error free (Andersen, et al., 1999). I also consider Realized GARCH model presented by (Hansen, et al., 2012) where a realized measure is used for modelling daily volatility of cryptocurrencies.

(Aalborg, et al., 2019) assess factors affecting return, volatility and trading volume of Bitcoin. They consider variety of variables including number of unique Bitcoin addresses and Google searches for Bitcoin. They utilize realized volatility measure computed from high-frequency data and discover that heterogeneous autoregressive model by (Corsi, 2009) is appropriate to model Bitcoin volatility and that addition of trading volume further improves this model.

GARCH-MIDAS[1] has been used extensively in previous studies for different purposes. (Conrad, et al., 2018) investigate impact of different indicators on volatility of Bitcoin. They conclude that Bitcoin volatility is inversely associated with US stock market volatility, but that it is strongly related to Baltic dry index which is a proxy of global economic activity. (Fang, et al., 2019) find that greater uncertainty in global economy increases hedging usefulness of Bitcoin. Higher global

[1] GARCH-MIDAS model proposed by (Engle, et al., 2013) decomposes volatility into long-term and short-term components. It provides the basis to consider effect of high and low frequency observations, and to evaluate impact of other indicators on volatility being studied.

economic uncertainty provides greater forecasting power of Bitcoin volatility, negatively affects correlation between Bitcoin and bond and positively affects correlations between Bitcoin and equities or commodities. Empirical results of (Fang, et al., 2019) show that if different economic uncertainty conditions are considered, hedging usefulness of Bitcoin is not significant. (Walther, et al., 2019) find Global Real Economic Activity, among factors under their investigation, to be the most relevant factor associated with volatility of cryptocurrencies, giving better volatility forecasts for bull and bear markets.

2.4 Multivariate Volatility

The main purpose of multivariate volatility modelling is to study the relationship between volatilities and co-volatilities in different markets or assets. Generally, multivariate models impose restrictions to limit number of parameters which need to be estimated and to ensure positivity of volatilities and symmetry of correlation or covariance matrix.

VEC model by (Bollerslev, et al., 1988) utilizes vector half operator to construct recursions for updates. Special cases of VEC model are DVEC, initially due to (Bollerslev, et al., 1988) in which the coefficient matrices are restricted to be diagonal and Baba, Engle, Kroner and Kraft (BEKK) model ensures positivity of volatility (Baba, et al., 1990).

Using BEKK-GARCH to estimate conditional correlations, (Klein, et al., 2018) analyze the relationship between cryptocurrencies and stock indices and commodities, and investigates hedge and safe-haven properties of cryptocurrencies compared to gold. With a similar method, (Beneki, et al., 2019) test volatility spillovers and hedging capabilities between Bitcoin and Ethereum. They investigate whether increased volatility from one of the currencies can be transferred to another one, arguing that a delayed volatility transmission between Bitcoin and Ethereum provides the basis for profitable trading strategies. They find that although Bitcoin and Ethereum exhibit some diversification capabilities in the beginning, capabilities tend to diminish over time.

Analyzing volatility co-movements and interdependencies between Bitcoin and Ethereum, (Katsiampa, 2019) utilizes Diagonal BEKK model and finds that volatility and correlation react to major news. Moreover, this study shows that Ether can be used as an effective hedge against Bitcoin. Using asymmetric BEKK-GARCH to investigate return, volatility and shock relations between Bitcoin and some stock indices, including clean energy, fossil fuel energy and technology companies, (Symitsi & Chalvatzis, 2018) investigates how Bitcoin can be used for diversification and portfolio management.

Another method of multivariate modelling, conditional correlation models are constructed by decomposing the covariance matrix into standard deviation matrix and correlation matrix. Many models have been proposed in the literature to focus on the specification of correlation matrix. The correlation matrix can be considered either constant or dynamic through time.

One of the subsets of conditional correlation models, Constant Conditional Correlation (CCC) model by (Bollerslev, 1990) assumes that correlation matrix remains unchanged during time, an assumption which is often unrealistic. Dynamic Conditional Correlation (DCC) of (Tse & Tsui, 2002) allows conditional correlation matrix to evolve over time while DCC of (Engle, 2002) permits conditional covariance matrix to vary during time.

(Creal, et al., 2012) propose Generalized Autoregressive Score (GAS) model for multivariate time varying volatilities and correlations. This model includes update based on score function for prediction. Moreover, this model allows capturing observations of outliers, and is suitable for heavy tailed distributions which are typically observed in Finance.

3. Methodology

In this section, I explain the models which are used in this study in the following order. Initially, descriptions related to univariate volatility models are provided. Thereafter, I provide explanations regarding multivariate models. In addition, I include explanations regarding information criterion AIC and BIC, and regarding the Diebold Mariano (Diebold & Mariano, 1995) test.

3.1 Univariate

In the analysis of time series gathered from different markets, I will utilize logarithmic returns which are defined as:

$$\Delta \ln P_t = \ln P_t - \ln P_{t-1} = \ln\left(\frac{P_t}{P_{t-1}}\right)$$

Where P_t denotes price of asset, in my case Bitcoin, at time t. Logarithmic return is preferred in finance as it is additive and believed to be more stationary, which is a paramount characteristic for a financial time series (Tsay, 2005). From now, I denote asset return series with y_t which can be rewritten as follows:

$$y_t = \sqrt{h_t}\varepsilon_t \quad , \quad \varepsilon_t \sim iid\left(0,1\right)$$

Alternatively, I can consider conditional distribution of y_t with respect to information available at time $t-1$ formally $y_t \mid Y_{t-1}$. Among different possible distributions for ε_t or $y_t \mid Y_{t-1}$, I choose Gaussian and Student's *t*, which are more common. I estimate parameters with maximum likelihood. For the Gaussian distribution, I can write:

$$y_t \mid Y_{t-1} \sim N(0, h_t)$$

$$f\left(y_t \mid Y_{t-1}\right) = \frac{1}{\sqrt{2\pi h_t}}\left(\frac{y_t^2}{h_t}\right)^{-1/2}$$

Log-likelihood function can be derived as:

$$L = \prod_{t=1}^{n} f\left(y_t \mid Y_{t-1}\right)$$

$$\log(L) = \sum_{t=1}^{n} l\left(y_t \mid Y_{t-1}\right)$$

$$l\left(y_t \mid Y_{t-1}\right) = -\frac{1}{2}\left(\log\left(2\pi\right) + \log\left(h_t\right) + \frac{y_t^2}{h_t}\right)$$

$$log(L) = \sum_{t=1}^{n} -\frac{1}{2}\left(\log\left(2\pi\right) + \log\left(h_t\right) + \frac{y_t^2}{h_t}\right)$$

If I consider Student's t distribution for conditional returns, I can follow the same procedure as in (Bollerslev, 1986) and write:

$$f\left(y_t \mid Y_{t-1}\right) = \frac{\Gamma\left(\nu + 1\!\!\diagup\!\!2\right)}{\Gamma\left(\nu\!\!\diagup\!\!2\right)\sqrt{\pi\left(\nu-2\right)h_t}}\left(1 + \frac{y_t^2}{\left(\nu-2\right)h_t}\right)^{-\left(\nu+1\!\!\diagup\!\!2\right)}$$

$$\log(L) = \sum_{t=1}^{n}\left(\log\left(\Gamma\left(\frac{\nu+1}{2}\right)\right) - \log\left(\Gamma\left(\frac{\nu}{2}\right)\right) - \frac{1}{2}\log\left(\pi\left(\nu-2\right)\right) - \frac{1}{2}\log\left(h_t\right) - \left(\frac{\nu+1}{2}\right)\log\left(1 + \frac{y_t^2}{\left(\nu-2\right)h_t}\right)\right)$$

To arrive at the maximum likelihood estimator for each assumption of density, I maximize log-likelihood functions defined above. To estimate the parameters of different models used in this study, I will maximize the log-likelihood function in which I substitute different filters for conditional variance h_t .

3.1.1 GARCH(1,1)

The first set of models used in this study is GARCH(1,1) with Gaussian and Student's t distributions. These models are used as the baseline for univariate. Filter equation for conditional variance in GARCH(1,1) is defined as:

$$h_t = \alpha_0 + \alpha_1 y_{t-1}^2 + \beta_1 h_{t-1}$$

In order to implement the above model, some restrictions are typically imposed to ensure, for example, that unconditional variance is finite. The restrictions are:

$$0 < \alpha_0 \quad , \quad 0 \le \alpha_1 \quad , \quad \beta_1 < 1 \quad , \quad \alpha_1 + \beta_1 < 1$$

The GARCH recursion is initialized with unconditional variance implied by the model. In case of GARCH(1,1) model, it can be shown that unconditional variance is equal to $Var\left(y_t\right)=\frac{\alpha_0}{1-\left(\alpha_1+\beta_1\right)}$.

3.1.2 GAS(1,1)

GAS(1,1) is the second model evaluated in this study. For this model, I can write:

$$h_{t+1}=\omega+A_1 s_t+B_1 h_t$$

$$s_t=S_t\cdot\nabla_t$$

In the above expressions, h_t stands for conditional variance, ∇_t denotes score w.r.t. to h_t, and S_t refers to inverse of Fisher information. The above expression for s_t allows for greater flexibility for GAS filters, since S_t can be specified in different ways. However, an optimal filter is derived by using inverse of Fisher information. For Gaussian distribution, the filter above simplifies to:

$$h_{t+1}=\omega+A_1\left(y_t^2-h_t\right)+B_1 h_t$$

As illustrated by (Creal, et al., 2013), GAS(1,1) with Normal distribution is equivalent to Gaussian GARCH(1,1) model, however, the coefficients are not exactly the same. It can be shown that $\alpha_0=\omega$, $\alpha_1=A_1$ and $\beta_1=B_1-A_1$. The equivalency does not extend to other distributions. As the updates s_t depend on the score function and Fisher information, assuming Student's t distribution for conditional density results in different update equation, as follows:

$$h_{t+1}=\omega+A_1\left(1+3\nu^{-1}\right)\cdot\left(\frac{\left(1+\nu^{-1}\right)}{\left(1-2\nu^{-1}\right)\cdot\left(\left(1+\nu^{-1}y_t^2\right)\Big/\left(1-2\nu^{-1}\right)h_t\right)}y_t^2-h_t\right)+B_1 h_t$$

Which is clearly different from the GARCH(1,1) model. While GARCH(1,1) considers the same update for Gaussian and Student's t distributions, GAS(1,1) updates are structured to dampen contributions from observations from tails of distribution. This filter can capture observations from heavy tails of distribution and can absorb outliers, leading to improved model fit. In order to estimate the parameters, following restrictions are typically applied:

$$0 < \omega \ , \ 0 \le A_1, B_1 < 1 \ , \ A_1 + B_1 < 1$$

3.1.3 Realized GARCH

The next univariate model that I consider is the Realized GARCH model with log linear specification (Hansen, et al., 2012). Realized GARCH models relate the observed realized measure to the latent volatility through measurement equation, in which a leverage function can be included to consider asymmetric response to shocks.

Closely following (Hansen, et al., 2012) the filter and measurement equations for log linear specification are as follows:

$$h_t = \exp\left(\omega + \beta \log\left(h_{t-1}\right) + \gamma \log\left(x_{t-1}\right)\right)$$

$$\log\left(x_t\right) = \xi + \varphi \log(h_t) + \tau\left(\varepsilon_t\right) + u_t$$

In the above equation, x_t represents realized measure which is computed at high frequency. As I can see in the filter equation, rather than squared return in GARCH and GAS models, Realized GARCH model includes realized measure for prediction of conditional variance. In this study, x_t is Realized Variance and is defined as:

$$x_t = \sum_{i=1}^{m}\left(\log\left(P_{i,t}\right) - \log\left(P_{i-1,t}\right)\right)^2 = \sum_{i=1}^{m} y_{i,t}{}^2$$

In addition, $\tau\left(\varepsilon_t\right) = \tau_1\varepsilon_t + \tau_2\left(\varepsilon_t^2 - 1\right)$, called leverage function, incorporates the effect of negative returns on future volatility. Leverage functions can be written using Hermite polynomials which are typically written as:

$$\tau\left(z_t\right) = \tau_1 z + \tau_2\left(z_t^2 - 1\right) + \tau_3\left(z_t^3 - 3z\right) + \ldots$$

However, as (Hansen, et al., 2012) argue, the polynomial of order two is both sufficient and convenient as it ensures $\mathrm{E}\left(\tau\left(z_t\right)\right) = 0$ for any process z_t which has $\mathrm{E}\left(z_t\right) = 0$ and $Var\left(z_t\right) = 1$. In this study, Realized GARCH models are considered in two different ways. Firstly, I simply estimate the model without leverage function, and secondly, I estimate the model including leverage function to achieve a model for analyzing asymmetric volatility.

With regard to estimation, I follow (Hansen, et al., 2012) and assume independent distributions of filter and measurement equations. Therefore, joint conditional distribution can be decomposed to multiplication of densities. Then, by taking logarithm, the log-likelihood function can be written as the sum of the log likelihood functions. Formally, I can write as illustrated by Hansen et al. (2012) as follows:

$$\log L\left(\{y_t, x_t\}_{t=1}^{n}; \theta\right) = \sum_{t=1}^{n} \log f\left(y_t, x_t \mid Y_{t-1}\right)$$

$$f\left(y_t, x_t \mid Y_{t-1}\right) = f\left(y_t \mid Y_{t-1}\right) f\left(x_t \mid y_t, Y_{t-1}\right)$$

$$l\left(y, x\right) = -\frac{1}{2}\sum_{t=1}^{n}\left[\log(2\pi) + \log\left(h_t\right) + \frac{y_t^2}{h_t}\right] + -\frac{1}{2}\sum_{t=1}^{n}\left[\log(2\pi) + \log\left(\sigma_u^2\right) + \frac{u_t^2}{\sigma_u^2}\right]$$

Therefore, in case of Realized GARCH model the above function will be maximized to estimate the parameters of the model for Gaussian distribution assumption of measurement and filter equations. Moreover, I investigate Realized GARCH for Student's t for which I propose that the log-likelihood is:

$$\begin{aligned} l\left(y, x\right) = \sum_{t=1}^{n}\Bigg(&\log\left(\Gamma\left(\frac{\nu_1+1}{2}\right)\right) - \log\left(\Gamma\left(\frac{\nu_1}{2}\right)\right) - \frac{1}{2}\log\left(\pi\left(\nu_1-2\right)\right) - \frac{1}{2}\log\left(h_t\right) - \left(\frac{\nu_1+1}{2}\right)\log\left(1 + \frac{y_t^2}{\left(\nu_1-2\right)h_t}\right)\Bigg) + \\ &+ \sum_{t=1}^{n}\left(\log\left(\Gamma\left(\frac{\nu_2+1}{2}\right)\right) - \log\left(\Gamma\left(\frac{\nu_2}{2}\right)\right) - \frac{1}{2}\log\left(\pi\left(\nu_2-2\right)\right) - \frac{1}{2}\log\left(\sigma_u^2\right) - \left(\frac{\nu_2+1}{2}\right)\log\left(1 + \frac{u_t^2}{\left(\nu_2-2\right)\sigma_u^2}\right)\right) \end{aligned}$$

3.1.4 GJR-GARCH

GJR-GARCH model by (Glosten, et al., 1993) allows for positive and negative returns to have a separate effect on the volatility. Motivated by (Baur & Dimpfl, 2018), I evaluate the effect of positive and negative returns on volatility of Bitcoin in different exchanges.

Filter equation for GJR-GARCH(1,1) is defined by the following equation:

$$h_t = \alpha_0 + \left(\alpha_1 + \alpha_1^{-} I_{(y_{t-1}<0)}\right) y_{t-1}^2 + \beta_1 h_{t-1}$$

Where $I_{(y_{t-1}<0)}$ denotes indicator function which takes value zero if the return in previous period is positive, and one if the return in previous period is negative. Therefore, the coefficient of squared return will be different for positive and negative returns, and investigation of asymmetric response of volatility becomes possible. For stock markets, α_1^- is expected to be positive, leading to greater increase in volatility after negative shocks. Restrictions to estimate the parameters in the above function are:

$$\alpha_0 > 0 \quad , \quad \alpha_1, \beta_1 \geq 0 \quad , \quad \alpha_1 + \alpha_1^- > 0$$

I investigate both Gaussian and Student's t distributions for GJR-GARCH model, and estimate the parameters.

3.1.5 EGARCH

(Nelson, 1991) introduces EGARCH model to account for asymmetric response of volatility to positive and negative shocks, referring to the asymmetric effect as leverage effect.
EGARCH(m,s) model in general is defined by the following:

$$y_t = \sqrt{h_t}\varepsilon_t \quad , \quad \varepsilon_t \sim NID(0,1)$$

$$\ln(h_t) = \omega + \frac{\alpha(L)}{\beta(L)} g(\varepsilon_{t-1}) = \omega + \frac{1+\beta_1 L + \cdots + \beta_{s-1} L^{s-1}}{1-\alpha_1 L - \cdots - \alpha_m L^m} g(\varepsilon_{t-1})$$

In which $g(\varepsilon_t)$ denotes weighted innovation and is given by

$$g(\varepsilon_t) = \theta\varepsilon_t + \gamma\left[|\varepsilon_t| - \mathrm{E}(|\varepsilon_t|)\right]$$

Moreover, for polynomials $\alpha(L)$ and $\beta(L)$ I have:

$$\alpha(L) = 0 \quad , \quad \beta(L) = 0 \Leftrightarrow |L| > 1$$

In this study, I consider EGARCH(1,1) as this option usually leads to optimal solution for financial time series.[2] In addition, I assume $\varepsilon_t \sim N(0,1)$, so I immediately conclude that $|\varepsilon_t|$ is half-normal for which I have $\mathrm{E}(|\varepsilon_t|) = \sqrt{\frac{2}{\pi}}$. Consequently, I can write filter equation as below:

$$\ln(h_t) = \omega(1-\alpha) + \alpha \ln(h_{t-1}) + \theta\varepsilon_{t-1} + \gamma\left[|\varepsilon_t| - \sqrt{\frac{2}{\pi}}\right]$$

From the above equation one can see that the coefficient for $|\varepsilon_t|$ in case of $\varepsilon_t > 0$ is $\gamma + \theta$ and in case of $\varepsilon_t < 0$ is $\gamma - \theta$. Therefore, to evaluate asymmetric response I will investigate the sign of coefficient θ. Negative θ implies that higher future volatility for negative returns, and positive θ relates higher future volatility to positive returns.

3.2 Multivariate

In multivariate part, my approach remains the same, and I estimate parameters by maximizing log-likelihood function, however, restrictions needed to ensure positivity of conditional variance and stationary process become more complex. In this section, I define vector y_t with dimension $N \times 1$ to denote multiple asset returns at time t. I have:

$$\mu_{t|t-1} = \mathrm{E}(y_t \mid Y_{t-1}), H_t = Var(y_t \mid Y_{t-1})$$

$$y_t = \mu_{t|t-1} + H_t^{1/2}\varepsilon_t$$

And assuming zero conditional return, the term $\mu_{t|t-1}$ vanishes and I arrive at:

$$y_t = H_t^{1/2}\varepsilon_t, y_t \mid Y_{t-1} \sim N(0, H_t)$$

The other assumptions are $\mathrm{E}(\varepsilon_t \mid Y_{t-1}) = 0$ and $\mathrm{E}(\varepsilon_t\varepsilon_t' \mid Y_{t-1}) = \mathrm{I}_N$ which are equivalent to standard white noise for univariate model.

[2] https://vlab.stern.nyu.edu/docs/volatility/EGARCH

3.2.1 GAS

In this study, I include two different specifications of GAS model: Equi-Correlation and constant correlation. In multivariate setting the filter equation is defined similar to univariate:

$$f_{t+1} = \omega + A_1 s_t + B_1 f_t$$

Where f_t is time varying factor which is in this research $\log\left(h_t\right)$. Equi-correlation structure is defined as:

$$R = \begin{pmatrix} \rho_{11} & \cdots & \rho_{1n} \\ \vdots & \ddots & \vdots \\ \rho_{n1} & \cdots & \rho_{nn} \end{pmatrix} = \begin{pmatrix} 1 & \cdots & \rho \\ \vdots & \ddots & \vdots \\ \rho & \cdots & 1 \end{pmatrix}$$

In contrast to above specification, I also define constant correlation structure as:

$$R = \begin{pmatrix} \rho_{11} & \rho_{12} & \rho_{13} \\ \rho_{21} & \rho_{22} & \rho_{23} \\ \rho_{31} & \rho_{32} & \rho_{33} \end{pmatrix} = \begin{pmatrix} 1 & \rho_{12} & \rho_{13} \\ \rho_{12} & 1 & \rho_{32} \\ \rho_{13} & \rho_{32} & 1 \end{pmatrix}$$

I follow (Koopman, et al., 2017) for derivations of the terms, and use similar equi-correlation structure. Therefore, the assumption is having constant correlation through time between all the exchanges. Equations related to this model are provided in the Appendix A. An important difference between this structure and the next one is that here I do not restrict matrices A and B to be diagonal, and their elements can be between -1 and +1.

I now provide the equations and assumptions related to constant correlation model. I follow (Creal, et al., 2012). Similarly to univariate part, I have $s_t = S_t \nabla_t$ in which $S_t = \mathrm{I}_{t|t-1}^{-1}$. In order to clarify equations used in this study for the multivariate GAS model, I briefly review some matrix operations. Expression $A \otimes B$ represents Kronecker product of matrices A and B, and I also denote Kronecker sum as $A \oplus B = \left(A \otimes B\right) + \left(B \otimes A\right)$. Operator $vec\left(A\right)$ vectorizes matrix A into a column vector, while $vech(A)$ vectorizes lower triangular part of matrix A. Duplication matrix D_k is defined such that $D_k vech(A) = vec\left(A\right)$.

With similar notation to (Creal, et al., 2012), I have:

$$f_t = \begin{pmatrix} \log\left(daig\left(D_t^2\right)\right) \\ vech\left(Q_t\right) \end{pmatrix}$$

$$D_t = diag\left(h_{11,t}^{1/2}, h_{22,t}^{1/2}, ..., h_{NN,t}^{1/2}\right)$$

$$H_t = D_t R D_t$$

In which $D_t = diag\left(h_{11,t}^{1/2}, h_{22,t}^{1/2}, ..., h_{NN,t}^{1/2}\right)$ is a diagonal matrix of standard deviations, and Q_t is a positive definite matrix used to compute correlation matrix: $R_t = \Delta_t^{-1} Q_t \Delta_t^{-1}$, in which Δ_t is a diagonal matrix with square root of diagonal elements of Q_t as its non-zero elements. Since I assume constant correlation, so Q_t and Δ_t may be written without the subscripts and I have $R = \Delta^{-1} Q \Delta^{-1}$.

In addition, I follow (Creal, et al., 2012) and define $\psi_t = \psi\left(f_t\right) = \frac{\partial vech\left(H_t\right)}{\partial f_t'}$, which is closely related to the chosen time varying variable f_t, to derive ∇_t and $\mathrm{I}_{t|t-1}^{-1}$. Initially, I present the intermediate terms for estimation of Student's t density. The Normal case is obtained by letting ν to go to infinity.

To derive ψ_t, I define elimination matrix B_k, for which $B_k \cdot vec\left(A\right) = vech\left(A\right)$. In addition W_{Dt} matrix is constructed from $k^2 \times k^2$ diagonal matrix $diag\left(0.5vec\left(D_t^{-1}\right)\right)$ and eliminating columns containing only zeros, and selection matrix S_D is defined as $\log\left(daig\left(D_t^2\right)\right) = S_D f_t$. For the specification of f_t given above, (Creal, et al., 2013) show that ψ_t is given by the following equation:

$$\psi_t = B_k\left(\mathrm{I} \oplus D_t R_t\right) W_{Dt} D_t^2 S_D$$

Then, the score and fisher is given by the following two equations:

$$\nabla_t = \frac{1}{2}\psi_t' D_k' \Sigma_{t\otimes}^{-1}\left[\bar{\nu}\, y_{t\otimes} - vec\left(\Sigma_t\right)\right]$$

$$I_{t|t-1} = \frac{1}{4}\psi_t{}' D_k{}' J_{t\otimes}{}' \left[\bar{\nu} G - vec(\mathrm{I}) vec(\mathrm{I})' \right] J_{t\otimes} D_k \psi_t$$

where $\bar{\nu} = \dfrac{\nu + N}{\nu + y_t H_t^{-1} y_t{}'}$ and N denotes number of exchanges. Moreover, J_t is implicitly defined by $\sum_t^{-1} = J_t{}' J_t$ and it can be obtained with various matrix decomposition techniques. In this study, I use Cholesky decomposition to compute J_t.

In addition, matrix G is defined by the following equation:

$$G\left[(i-1)\cdot k + l, (j-1)\cdot k + m\right] = \delta_{ij}\delta_{lm} + \delta_{il}\delta_{jm} + \delta_{im}\delta_{jl}$$

In the above equation, δ_{ij} denotes the Kronecker delta which is equal to one if $i = j$ and zero otherwise. In order, to estimate this model, I impose similar restrictions to those suggested by (Creal, et al., 2012)For simplicity, I assume matrices A and B are diagonal, with $N+1$ parameters to estimate for each matrix which are denoted by $a_1, a_2, ..., a_{N+1}$ and $b_1, b_2, ..., b_{N+1}$. The first N elements of each series are placed on the first N diagonal elements, the remaining diagonal elements are substituted by the element $N+1$. It should be noted that first N diagonal elements of each matrix is related to $\log\left(daig\left(D_t^2\right)\right)$ in my decomposition of f_t, and the other elements which are equal to a_{N+1} and b_{N+1} in A and B respectively are related to $vech\left(Q_t\right)$. What is more, I must ensure $1 \geq B \geq A \geq 0$, therefore, I need to satisfy:

$$1 \geq a_1, a_2, ..., a_{N+1} \geq 0 \ \ , \ 1 \geq b_1, b_2, ..., b_{N+1} \geq 0$$

In addition to restrictions imposed on A and B, there is another constraint for ω. Considering definitions provided for matrices Q and R, it can be seen that multiplying all elements of Q results in the same R. Therefore, elements of ω which are related to diagonal elements of Q in its $vech$ decomposition are restricted to be equal to one. Furthermore, I impose restrictions on elements of matrix R to remain between -1 and +1. Applying these constraints decreases number of parameters needed to be estimated and also ensures appropriate results from the model.

3.3 Model Selection

3.3.1 Information Criteria

I use information criteria to select a model with best performance among a set of candidates. I investigate in sample performance of different models with respect to both Akaike Information Criterion (AIC) and Bayesian Information Criterion (BIC). Information criteria are composed by an inverse measure of fit and an increasing function dependent on the number of parameters estimated.

The intuition behind the information criterion is to find the best compromise between fit and parsimony among the set of candidates. The preferred model is the one with minimum information criterion in both AIC and BIC. The formula for calculation of AIC and BIC are as follows:

$$AIC = -2\log(\hat{L}) + 2k \quad , \quad BIC = -2\log(\hat{L}) + k \cdot \log(n)$$

In the above equations $\hat{L}$ denotes the maximum value of likelihood function, k denotes the number of parameters estimated by the model and n refers to the number of observations. Clearly from the equations above, I can see that increasing number of parameters estimated by the model penalizes both AIC and BIC, leading to higher information criterion, while increasing the number of observations only affects and penalizes BIC, leading to heavier penalty for BIC.

3.3.2 MSE and Diebold Mariano Test

I also compare out-of-sample forecasts of different models in an expanding window analysis. All the univariate models proposed in this study, provide out-of-sample forecast. Therefore, the forecast of models can be compared to observed data in a pseudo out-of-sample exercise.

After estimating models for a window, and capturing the forecast for the following day, I estimate the model again after extending the estimation sample to include an additional return and repeat the process. Therefore, I have a series of forecasts for each of the models included in this study, predictions that I can compare with observed data and for which I can calculate the error of forecast. Forecast error is defined as:

$$e_{it} = \hat{\sigma}_{it} - \sigma_t$$

In which $\hat{\sigma}_{it}$ denotes prediction of volatility from model i at time t and σ_t is the actual conditional volatility. Since actual conditional volatility is not easy to estimate, I will use absolute returns $|y_t|$ as a proxy. In order to compare forecast error of different models, I calculate mean square error (MSE) as loss function for each model. This quantity is calculated as follows:

$$MSE = \frac{1}{n}\sum_{t=1}^{n}\left(\hat{\sigma}_{it} - \sigma_t\right)^2$$

Clearly, best performing model is the one with minimum MSE. Furthermore, taking square of errors provides higher weight for greater errors. However, in order to conclude about performances, I need to perform statistical test. (Diebold & Mariano, 1995) propose DM test statistic which is utilized to differentiate performances of different models. DM tests whether the forecast errors are statistically significant.

Loss function for DM test is defined as:

$$d_t = e_{it}^2 - e_{jt}^2$$

One shortcoming of this function is symmetric behavior for over and under estimation. Since I am considering for one period out of sample forecast I follow definitions of (Diebold & Mariano, 1995), and write test statistic, together with null and alternative hypothesis as follows:

$$H_0 : \mathrm{E}\left(d_t\right) = \bar{d} = 0 \;\;,\;\; H_1 : \mathrm{E}\left(d_t\right) = \bar{d} \neq 0$$

$$DM = \frac{\bar{d}}{\sqrt{\mathrm{var}\left(d_t\right)/T}} \sim \mathrm{N}\left(0,1\right)$$

In this study, I consider 5% significance level for the above test statistic and perform the test. In order to differentiate performance, I first perform DM test to see whether the series of errors are statistically different. If I find statistical evidence of different processes, I choose the one with least MSE as the best performing process. In addition it must be mentioned that this test provides the opportunity to compare models that use realized measures with other models. Since realized models include sum of two 7 likelihood functions, they cannot be compared with other models with AIC and BIC.

4. Data

In this section, firstly the general approach for processing high frequency data is explained, and secondly modifications for missing values are described. I gather high frequency data sets through different source and process them using mapper and reducer functions in Matlab to obtain daily log price, daily log return and daily realized variance for five minute intervals. Moreover, the number of five minute observations for each day is computed. I used five minute intervals in order to avoid market microstructure noise, however, I did not check the results under smaller or larger intervals.

In the first step, data sets are resampled at five minute intervals, and in each interval the last observation is taken for the 'closing' price of the interval. Next, I sum up realized measures for each day, and take the last price of each day. I consider 00:00 (UTC) as the start of a new day. I study three different exchanges which are Bitstamp, Bitfinex and Coinbase.

Data set for Bitstamp is entirely downloaded from bitcoincharts.com, and processed with the above mentioned method. The data set for Coinbase is downloaded entirely form Kaggle[3] and contains observations from late January 2015 to January 2019.

However, Bitfinex faced cyber-attack from August 3rd 2016 to August 9th 2016 which led to its servers being offline then. Therefore, there are no observations for this period for this exchange. This limited the time span of empirical study. I define the time period of this study from August 10th 2016 to January 7th 2019.

Data on Bitfinex suffers from further issues, and requires more modifications. The final data set for Bitfinex is created using two different sources. Initially, data set available on Kaggle[4] is processed, and it contains missing observations. Thus, I incorporate hourly data from cryptodatadownload.com for the missing days. The intervals in which the hourly data is incorporated are from February 22nd 2018 to March 5th 2018, and from October 28th 2017 to November 9th 2017.

[3] https://www.kaggle.com/mczielinski/bitcoin-historical-data/data#coinbaseUSD_1-min_data_2014-12-01_to_2019-01-09.csv

[4] https://www.kaggle.com/tencars/392-crypto-currency-pairs-at-minute-resolution

In total, I have missing observations for 26 days, while the time period of this study spans 880 days. I expect that this small number of days with missing 5 minute returns to have a small impact on the results for models using realized measures. In addition, it must be mentioned that the missing observations do not affect the results of other studies, but impact only the realized models for this specific exchange.

Figure 1 depicts relevant information for Coinbase while similar plots for other exchanges are provided in the appendix. From Figure 1, I can see spikes around January 2018, when the price bubble started to disappear. Moreover, as the price was increasing during 2017, volatility of the market experienced some sudden increases.

Additionally, in the third panel realized volatility of market illustrates spikes around January 2018. Furthermore, in the fourth panel, I can see longer right tail for the distribution of realized volatility, an observation referring to extremely volatile days and riskiness of investing in Bitcoin. Second and third subplots, which depict absolute return and realized volatility, exhibit volatility clustering for Bitcoin. In addition, I provide plot of log realized volatility which is similar to Normal distribution, and it better depicts heavy tail of distribution

In addition, the realized volatility of market illustrates spike around January 2018, and its distribution displays longer right tail, indicating presence of highly volatile days. In general, I see volatility clustering in both realized volatility and volatility of return. In addition, I provide plot or log realized volatility which exhibits closer behavior to Normal distribution, and it better depicts heavy tail of distribution.

As shown in the Table 1, average daily return for different exchanges is around 0.2%, but it is statistically insignificantly different from zero. Moreover, unconditional standard deviation for different exchanges is 4%, and the correlations are approximately equal to one and are statistically significant.

Negative skewness for returns provides evidence of longer left tail than right tail. Kurtosis is higher than 6 which indicates evidence for existence of heavy tails or outliers. Moreover, based on Jarque-Bera test (denoted by p_{JB}) I reject the null hypothesis that the data is drawn from a normal distribution. It must be mentioned that Jarque-Bera tests simultaneously skewness and kurtosis of the distribution, and compares it with with a normal distribution.

Table 1: Return summary of all exchanges

Table 1 shows the summary of returns for all the markets. μ refers to unconditional mean over the sample period and p_μ denotes p-value of statistical significance of μ. In addition, ρ refers to correlation, and its indices 1,2 and 3 respectively refer to Coinbase, Bitfinex and Bitstamp. p_ρ refers to p-value of test with null hypothesis that correlation is equal to zero, and p_{JB} refers to p-value of Jarque-Bera test.

	NumObs	*Min*	*Max*	μ	p_μ	σ	ρ	p_ρ	*Skewness*	*Kurtosis*	p_{JB}
Coinbase	880.00	-0.18	0.22	0.217%	0.13	4%	$\rho_{12} = 0.98$	0.00	-0.07	6.33	0.001
Bitfinex	880.00	-0.19	0.23	0.228%	0.12	4%	$\rho_{23} = 0.99$	0.00	-0.18	6.17	0.001
Bitstamp	880.00	-0.18	0.22	0.217%	0.13	4%	$\rho_{31} = 0.99$	0.00	-0.18	6.16	0.001

Table 2 provides a similar summary for realized volatility of each exchange. Correlations are close to one, skewness values are estimated to be greater than zero, providing evidence of longer right tail and high realized volatility observations. Kurtosis ranges from 9.95 to 13.7, showing existence of heavy tails and outliers.

Table 2: Realized Volatility Summary

Table 2 shows summary of Realized Volatility for all the markets. μ refers to unconditional mean over the sample period and p_μ denotes p-value of statistical significance of μ. In addition, ρ refers to correlation, and its indices 1,2 and 3 respectively refer to Coinbase, Bitfinex and Bitstamp. p_ρ refers to p-value of test with null hypothesis that correlation is equal to zero, and p_{JB} refers to p-value of Jarque-Bera test.

	NumObs	*Min*	*Max*	μ	p_μ	σ	ρ	p_ρ	*Skewness*	*Kurtosis*	p_{JB}
Coinbase	880.00	0.00	0.29	4%	0.00	3%	$\rho_{12} = 0.97$	0.00	2.55	13.70	0.00
Bitfinex	880.00	0.00	0.28	4%	0.00	3%	$\rho_{23} = 0.97$	0.00	2.23	11.04	0.00
Bitstamp	880.00	0.01	0.24	4%	0.00	3%	$\rho_{31} = 0.97$	0.00	2.08	9.95	0.00

Next, I investigate characteristics of data. Figure 1 depicts autocorrelation of returns, absolute returns and realized volatility for Coinbase. As expected, there is no significant autocorrelation between lags of returns, while absolute return, a proxy of market volatility, provides evidence of dependence. The autocorrelation does not decay geometrically and provides evidence of heteroskedasticity. Similarly, the plot of realized volatility shows serial dependence as expected.

In the rest of this paper, I will provide some of the results only for Coinbase as it was the biggest retail exchange in the time period of my empirical study. However, it must be mentioned that I observe similar results for other markets as well. For some analyses, I also include results for Bitfinex in the main text since it is suspected to be behind price manipulations during 2017.

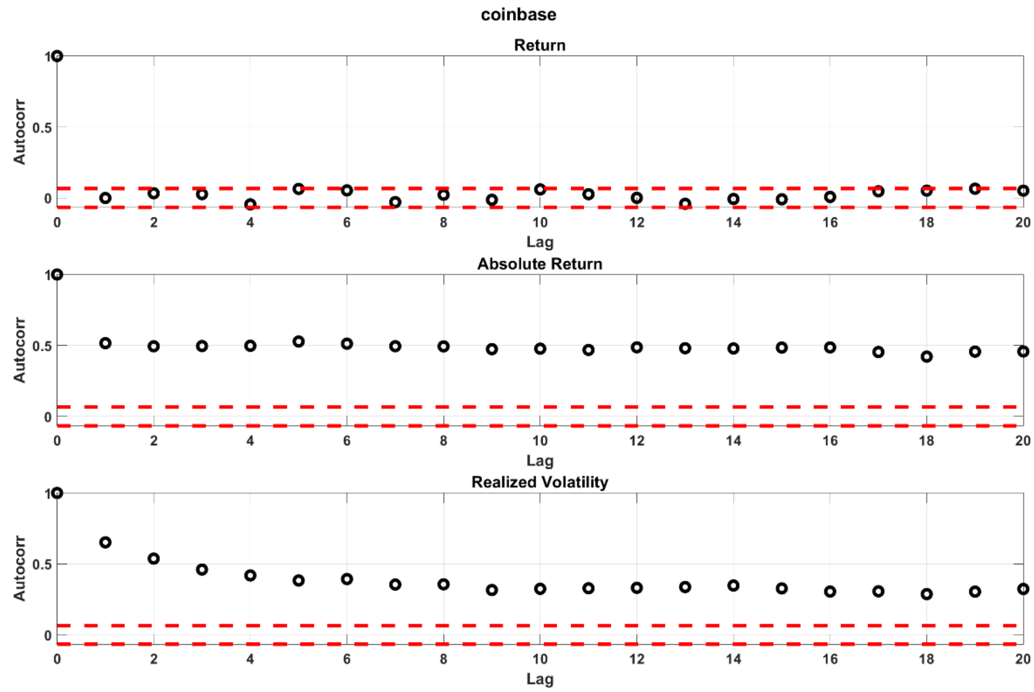

Figure 1: Autocorrelation for Coinbase

Figure 1 shows the autocorrelation results for return, absolute return and realized volatility of Coinbase. Red dashes show the rejection area at 5% significance level. In first panel, I assess appropriateness of AR process for modelling return, while in second and third panels, I explore suitability of conditional heteroskedasticity models for modelling volatility.

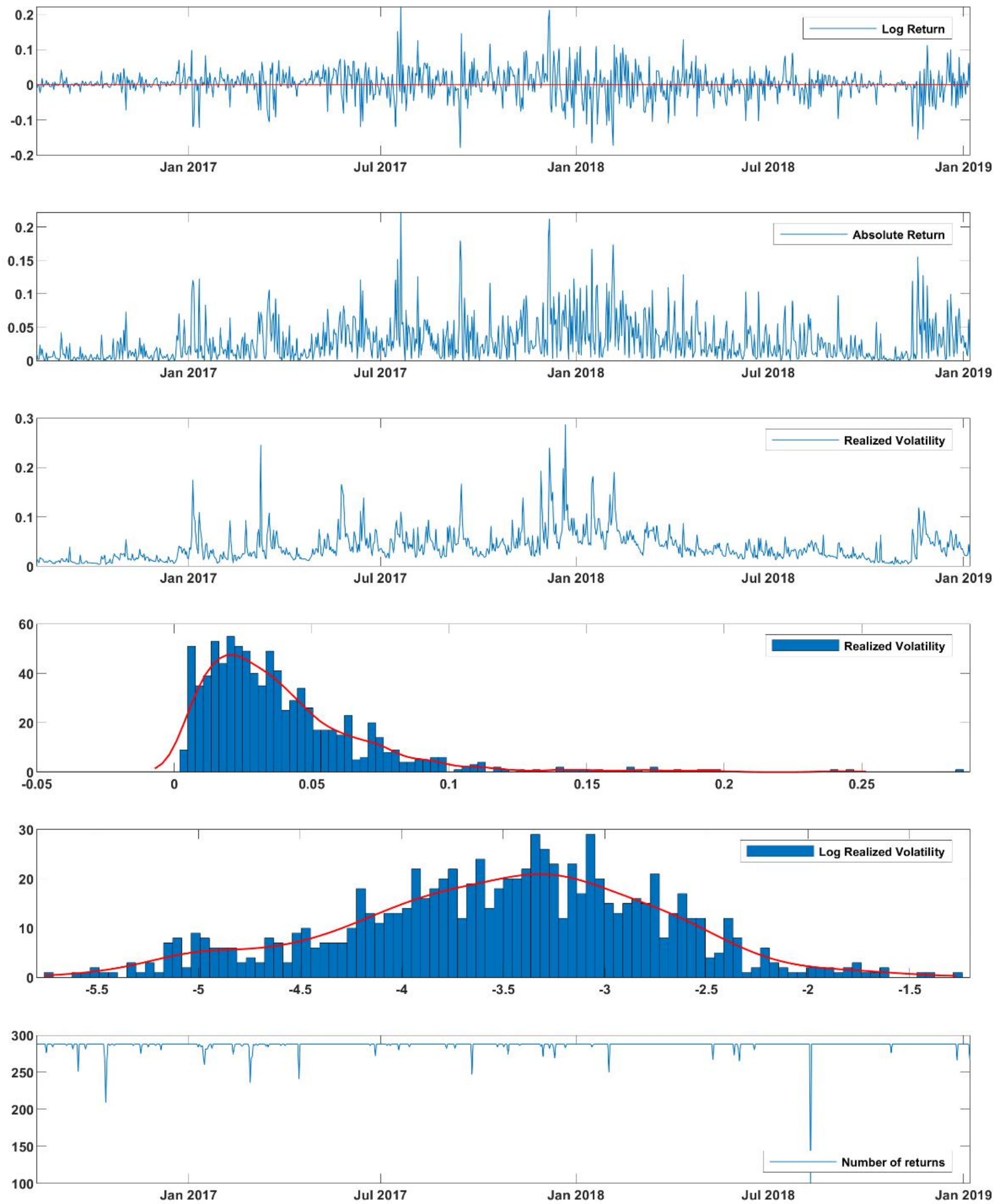

Figure 2: Coinbase Summary

Figure 2 provides visual description of the data of Coinbase. Return series is depicted in panel 1 in which red line shows zero mean. Panels 2 and 3 depict volatility clustering in the market. Red lines in panels 4 and 5 show the kernel density fitted to realized volatility and log realized volatility. Panel 6 shows the number of observations per day which should be 288 if there are no missing observations.

5. Results

5.1 Univaraite Models

In this section, I present results of univariate modelling for different exchanges. I present the results for Coinbase, which is the largest exchange in the period of this study, in the main text, and similar results for other exchanges are given in the appendix. I compare different models, and I provide a comparative analysis of results for the three exchanges. For representation purposes, models' names are modified to become shorter for the tables, and all the abbreviations are shown in Table 3.

Table 3: Abbreviations used in the study for representation purposes

Table 3 shows the abbreviations used in the tables of this study, and provides their descriptions. This table can be a reference point for reading the other tables in which results of models are presented.

Abbreviation	*Description*
NGC	Normal GARCH
NGS	Normal GAS
TGC	t-student GARCH
TGS	T-GAS
NRL	Normal Realized with Log transformation
TRL	t-student Realized with Log transformation
NRLL	Normal Realized with Leverage and Log transformation
TRLL	t-student Realized with Leverage and Log transformation
NGJR	Normal GJR
TGJR	t-student GJR
EGC	E GARCH
Normal-Equi	Normal Equi Correlation structure
t-Equi	t-student Equi Correlation structure
ConstRN	Normal Constant Correlation
ConstRt	t-student Constant Correlation

Figure 3 displays results of different models without leverage for Coinbase. First panel depicts the convergence of Normal GARCH and Normal GAS models. This is not surprising as the Normal GAS is equivalent to Normal GARCH. Second subplot depicts t-GARCH and t-GAS models, for which I can observe differences in predictions. Forecasts generated by t-GAS are in some periods higher than those of t-GARCH. This can be attributed to utilization of score in the updates for t-

GAS model which improves the predictions. Specifically predictions around January 2018 when the price bubble disappeared are higher for t-GAS.

Third panel in Figure 3, shows the Normal and Student's t Realized GARCH models. Predictions of volatility with this class of models are in general higher than GARCH and GAS models, an observation closely related to inclusion of realized measure for forecasting and possessing larger information set.

It must be mentioned that appearance and disappearance of some of the spikes in the predictions is may be attributed to misspecification of density in the observation equation. For instance, on January 2018, I observe a spike which can be due to either explosion of price bubble or a realization of tail risk. Considering available information, I conclude that this observation is related to explosion of price bubble, and that this finding shows advantage of using t-GAS.

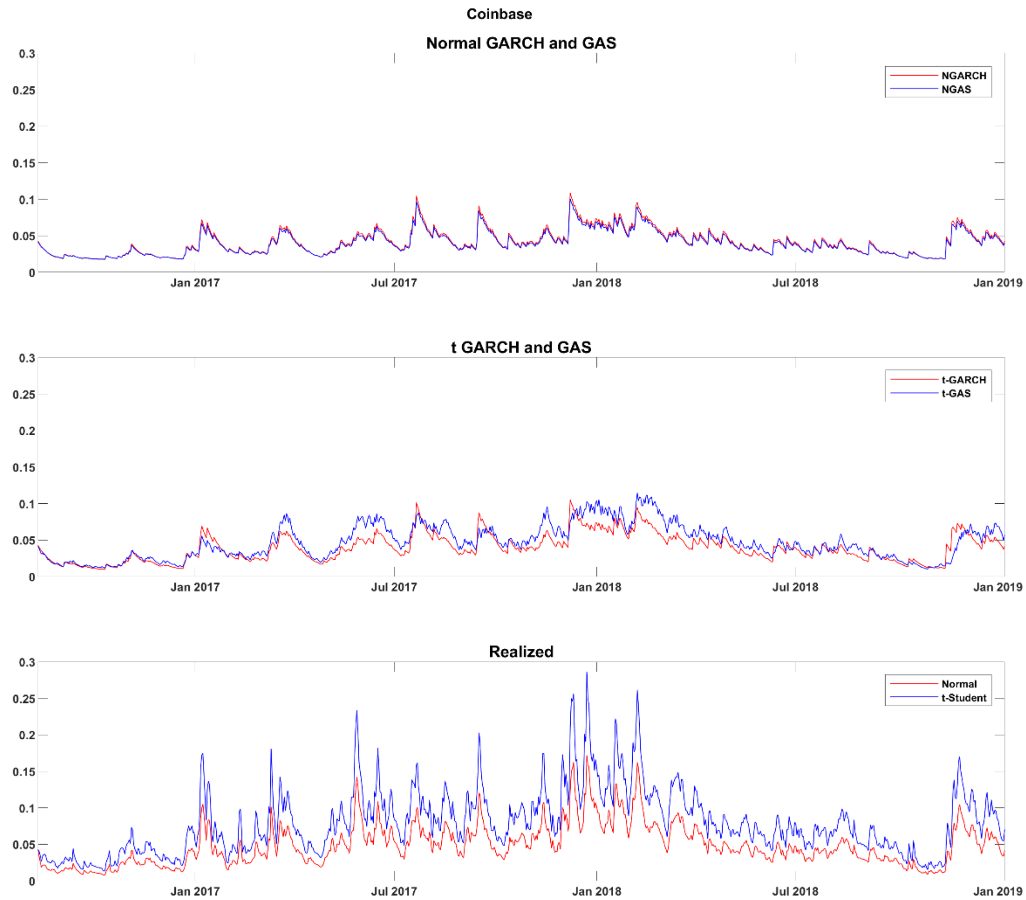

Figure 3: Coinbase no leverage models

Figure 3 shows the predictions of Normal GARCH and GAS, Student's t GARCH and t-GAS, and Normal and Student's t realized GARCH model and provides the basis for comparing these predictions.

Figure 4 depicts comparison of different Student's t models without leverage function and displays more spikes in realized model than in t-GARCH and t-GAS models. These spikes can be due to higher realized measures in the period. Moreover, I can observe a spike before January 2019 when realized model and t-GARCH model depict high forecast while t-GAS absorbs this spike as an outlier.

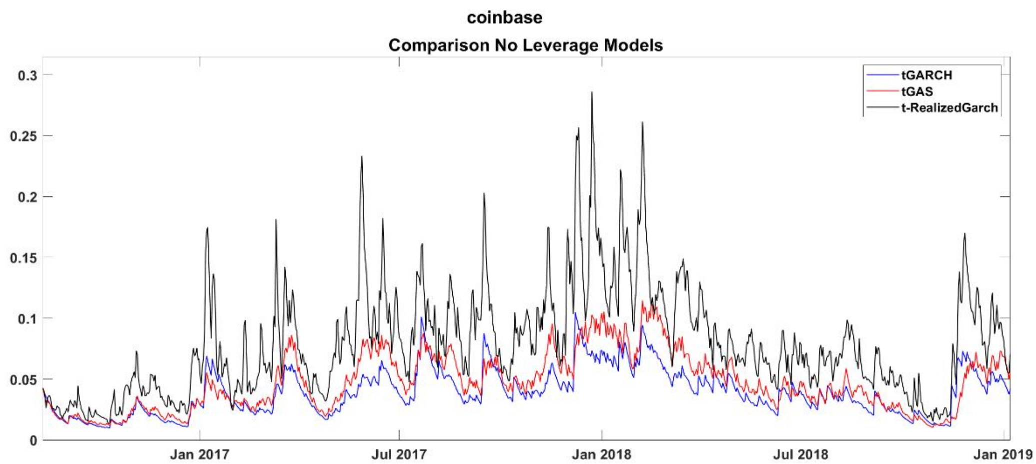

Figure 4: Coinbase comparison of no leverage models

Figure 4 shows predictions of different models which do not include leverage with student's t distribution. This figure provides the basis for comparison of forecasts between models.

In all the comparisons, I can see that changing the assumption of density affects levels and dynamics of predictions. However, comparison between t-GARCH and t-GAS depicts more differences between two models. Although t-GAS generates higher predictions than t-GARCH, its forecasts sometimes fall below the t-GARCH for realizations of outliers, and sometimes remain above t-GARCH because new impact curve converges to zero for t-GAS.

Observing differences between predictions t-GARCH and t-GAS, I would like to highlight the spikes in realized models. As I can see when I observe a spike in the realized model, t-GARCH shows the spike simultaneously, but t-GAS initially absorbs the shock. Indeed, it takes more observations for t-GAS to adjust to a new level of volatility. Since Realized GARCH utilizes same procedure, it reflects jumps similar to GARCH model.

Along with above, I can see that sudden increases and decreases around January 2018 in predictions of realized model are follow by GARCH model, however, t-GAS remains relatively stable and above t-GARCH in the following period. I would like to highlight other characteristics of t-GAS: (i) it provides generally smoother path of predictions and (ii) its paths do not contain prolonged periods of geometric decay. These characteristics are due to the efficient update included in this model.

Figure 5 depicts comparison of different models which include leverage. First panel shows comparison of Gaussian and Student's t GJR models. Assumption of Student's t density generates higher predictions for volatility and produces greater spikes in mid and late 2017 and early 2018.

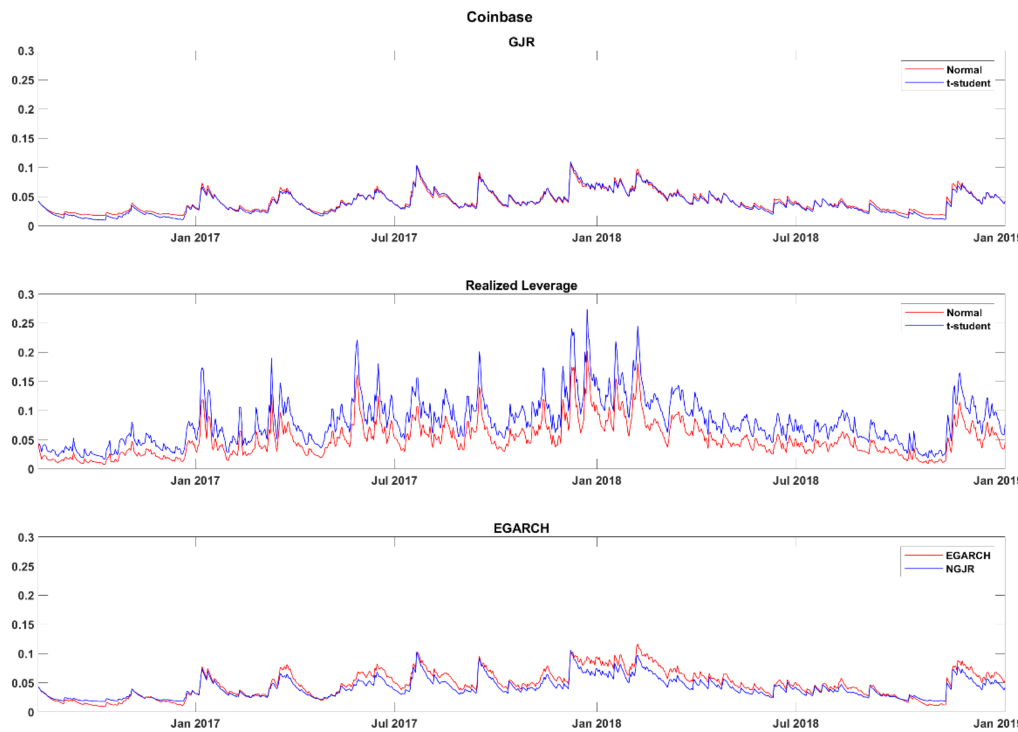

Figure 5: Coinbase models with leverage

Figure 5 shows the forecasts of models which include leverage function. In subplots 1 and 2, I provide results of Normal and student's t GJR and Realized GARCH with Leverage, and in subplot 3, I compare the forecasts of EGARCH and Normal GJR model.

Second panel in Figure 5 shows comparison of Gaussian and Student's t distributions for Realized GARCH with leverage function. I can see that Student's t density provides overall higher forecasts and more peaked spikes, a finding related to estimated degrees of freedom which will be followed in Table 4. Third panel in Figure 5 shows comparison between EGARCH model and Gaussian

GJR, both models having Gaussian assumption for density. This subplot shows that EGARCH model generates higher predictions and spikes than Normal GJR.

Figure 6 depicts results of Normal GARCH, t-GAS and Realized GARCH with Student's t distribution for all the exchanges. None of the models in this figure include leverage. From Figure 6, I can see that predictions for all markets have a similar trend. There are not substantial differences when comparing based on Normal GARCH and t-GAS. However, specification of Realized GARCH with Student's t emphasizes differences, exhibiting highest predicted volatility for Coinbase and lowest predicted volatility for Bitstamp. To further check this result, I check the plots for models which include leverage function with Student's t density.

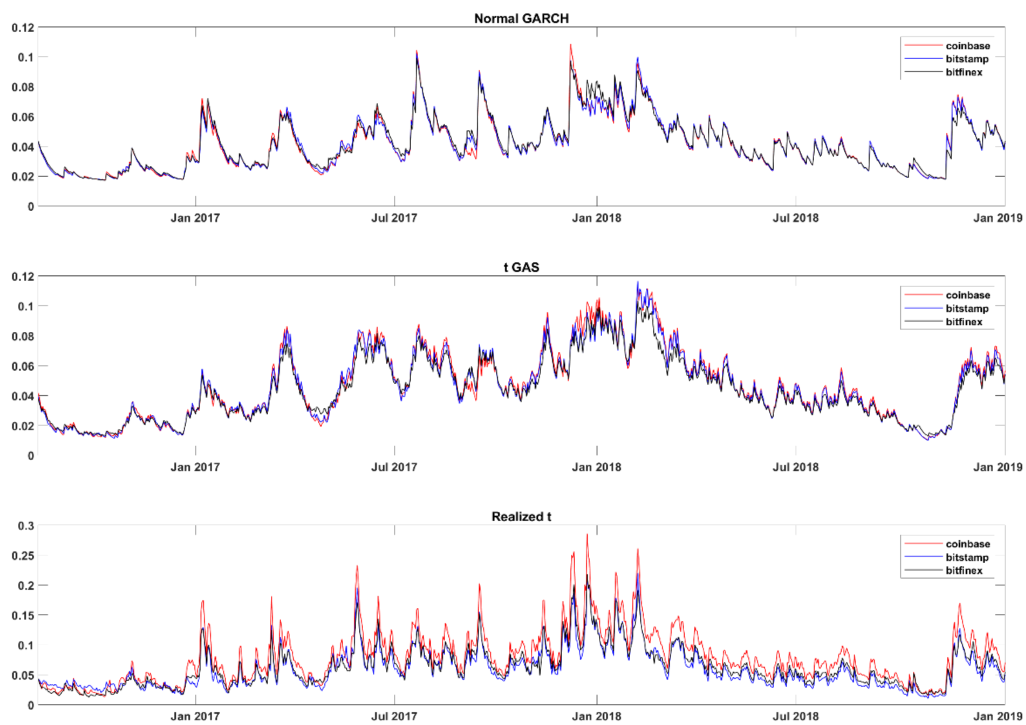

Figure 6: All exchanges no leverage

Figure 6 shows predictions of Normal GARCH, t-GAS and Realized GARCH with student's t distribution for all the markets. In each subplot forecasts of all the markets are provided and compared. Difference in forecasts is more emphasized in subplot 3, and it depicts that Coinbase has the highest and Bitstamp hast the lowest volatility forecasts.

Figure 7 depicts differences of markets given by Student's t density assumption of GJR and Realized GARCH with leverage. In Figure 7, I can still see that forecasts for Coinbase are the highest and for Bitstamp are the lowest. However, this plot shows closer predictions for Coinbase and Bitfinex, and the difference between forecasts of these two markets and forecasts of Bitstamp is considerable. Estimated degrees of freedom are given in Table 4 for Student's t density of different markets, providing evidence that Coinbase has the lowest value in all models among markets. Therefore, estimated degrees of freedom can be one reason for appearance of Coinbase above other markets.

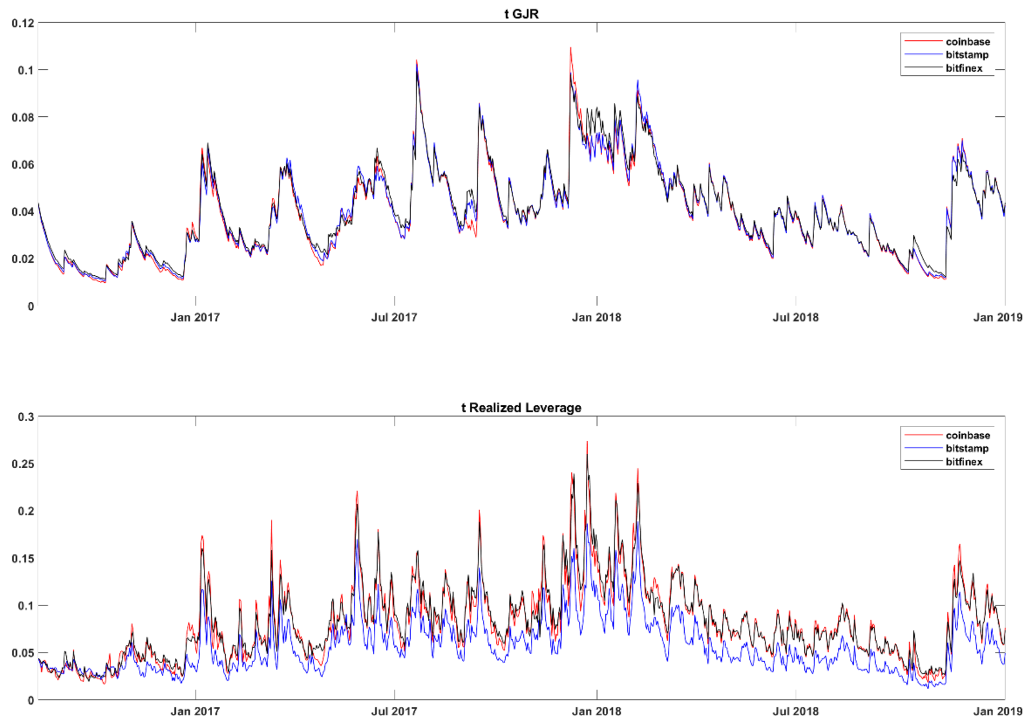

Figure 7: Leverage models all exchanges

Figure 7 shows the comparison of predicted volatilities of different markets with respect to models which include leverage and have student's t distribution. It can be seen that Bitstamp has the lowest volatility among the markets.

Table 4 shows the values of log likelihood, AIC and BIC, which are provided in average contributions. Estimation results show that among GARCH and GAS models, t-GAS outperforms other models for all exchanges. Among GJR and EGARCH models Student's t GJR model is the most appropriate model. These results are provided for the time period of this study, and it must be noted that the time span of data set includes the dramatic price rise of Bitcoin in 2017 and bubble price explosion of early 2018.

Realized models are not comparable in terms of neither log-likelihood nor AIC and BIC with other models. This fact is due to different definition of log-likelihood for realized models, for which I take into account log-likelihood for both measurement and filter equations. Therefore, comparing log-likelihood of these models with other models is not appropriate. Among realized models, the most suitable in terms of measurement criterion is Student's t with leverage.

Models are constructed by constraining number of degrees of freedom to be greater than 2, and I can see that number of degrees of freedom estimated range between 2 and 4.02 in all the exchanges for all the models, leading us to conclude that the conditional distributions are heavy tailed. Another interesting fact about the results is that moving from Gaussian distribution to Student's t distribution improves AIC and BIC criterion in all the exchanges, providing evidence to conclude that between Gaussian and Student's t distributions, the latter is more appropriate.

Regarding leverage models, results show that in the period of this study, $\theta < 0$ for EGARCH model and $\tau_1 < 0$ and $\tau_2 > 0$ for the Realized GARCH model with leverage equation. Moreover, Table 4 provides $\alpha^- < 0$ for Student's t GJR and $\alpha^- > 0$ for Normal GJR model. As it was explained in the methodology section, results of estimating EGARCH, Normal GJR and all the realized models in all the markets are consistent with stock markets and asymmetric volatility response to shocks. However, TGJR provides evidence of inverse effect. Because of time constraint, I could not estimate standard errors, thus, I cannot assess significance of estimated parameters of different models.

Table 4: Univariate Results

Table 4 shows the estimated parameters together with values of log-likelihood, AIC and BIC, which are provided by dividing the original values by the number of observations. Log-likelihood, AIC and BIC values which belong to models with best in sample performance in each class of models are shown in bold.

	Model	*ω*	*α*	*β*	*γ*	*α⁻*	*θ*	*v₁*	*ξ*	*φ*	*τ₁*	*τ₂*	*v₂*	*LL*	*AIC*	*BIC*
Coinbase	*NGC*	4.31E-05	0.14	0.85										1.857	-3.708	-3.692
	NGS	4.35E-05	0.12	0.97										1.856	-3.705	-3.689
	TGC	8.75E-06	0.13	0.87				3.84						1.951	-3.892	-3.871
	TGS	1.63E-05	0.10	0.99				2.83						**1.952**	**-3.894**	**-3.873**
	NRL	2.8E-08		0.63	0.34				-0.59	1.01				0.491	-0.971	-0.944
	TRL	2.8E-01		0.55	0.38			2.23	-1.31	1.08			4.62	0.68	-1.344	-1.306
	NRLL	7.7E-08		0.51	0.44				-0.47	1.04	-0.08	0.13		0.603	-1.191	-1.153
	TRLL	1.9E-06		0.47	0.40			2.21	0.00	1.21	-0.37	0.90	3.00	**0.878**	**-1.735**	**-1.686**
	NGJR	4.4E-05	0.14	0.85		0.02								1.858	-3.706	-3.684
	TGJR	7.6E-06	0.14	0.87		-0.03		3.84						**1.951**	**-3.891**	**-3.864**
	EGC	9.1E-08	0.99		0.31		-0.03							1.816	-3.623	-3.602
Bitstamp	*NGC*	3.98E-05	0.14	0.85										1.853	-3.699	-3.683
	NGS	3.97E-05	0.12	0.98										1.852	-3.697	-3.681
	TGC	1.00E-05	0.13	0.87				3.93						1.937	-3.865	-3.843
	TGS	1.50E-05	0.10	0.99				2.91						**1.942**	**-3.876**	**-3.854**
	NRL	5.0E-08		0.58	0.40				-0.62	0.94				0.739	-1.466	-1.439
	TRL	3.6E-01		0.51	0.49			2.49	-1.35	0.91			4.95	0.912	-1.809	-1.771
	NRLL	6.1E-08		0.53	0.45				-0.47	0.97	-0.09	0.09		0.861	-1.707	-1.669
	TRLL	8.6E-09		0.46	0.48			2.56	-0.41	1.02	-0.22	0.35	2.67	**1.085**	**-2.149**	**-2.1**
	NGJR	4.1E-05	0.13	0.85		0.02								1.854	-3.698	-3.676
	TGJR	8.8E-06	0.14	0.87		-0.03		2.43						**1.937**	**-3.863**	**-3.836**
	EGC	7.5E-07	0.99		0.31		-0.03							1.823	-3.636	-3.615
Bitfinex	*NGC*	3.47E-05	0.13	0.86										1.841	-3.674	-3.658
	NGS	3.38E-05	0.11	0.98										1.84	-3.673	-3.656
	TGC	1.01E-05	0.12	0.88				4.02						1.912	-3.816	-3.794
	TGS	1.48E-05	0.09	0.99				3.20						**1.916**	**-3.823**	**-3.801**
	NRL	4.0E-07		0.62	0.35				-0.53	0.99				0.61	-1.209	-1.182
	TRL	5.6E-06		0.55	0.38			2.48	-0.55	1.10			4.86	0.758	-1.5	-1.462
	NRLL	3.9E-08		0.54	0.42				-0.29	1.03	-0.06	0.18		0.794	-1.572	-1.534
	TRLL	5.0E-07		0.53	0.36			2.22	0.33	1.24	-0.26	1.00	3.39	**0.957**	**-1.894**	**-1.846**
	NGJR	3.6E-05	0.12	0.86		0.01								1.841	-3.672	-3.651
	TGJR	9.3E-06	0.13	0.88		-0.02		4.02						**1.92**	**-3.828**	**-3.801**
	EGC	1.9E-06	0.99		0.23		-0.01							1.812	-3.616	-3.594

In order to compare models out-of-sample with MSE and DM test, I use an expanding window approach. The interval over which I compare models is the last 50 days of data set. I estimate parameters of each model by incorporating information available from beginning of my sample. I divide the analysis into two stages. First, I test whether performance of Gaussian and Student's t distributions for same classes of models is different, and at the same time compare the values of MSE for them. For instance, NGC is compared with TGC, and this comparison is given in the column 'NGCvsTGC'. In addition, I compare EGC with NGJR in column 'NGJRvsEGC'. Table 5 represents results of DM tests, and Table 6 illustrates results for comparison of MSE. In Table 6, TRUE indicates lower MSE for left side of 'vs' than MSE for right side of it. For example, 'TRUE' for all markets in column 'NGSvsTGS' shows that MSE of NGS is lower than that of TGS.

Table 5: DM test statistic

Table 5 shows DM test statistic. Each column depicts results of DM test between two models, whose names are given in the column header. Bolded values show that null hypothesis can be rejected at 5% significance level.

	NGCvsTGC	*NGSvsTGS*	*NRLvsTRL*	*NGJRvsTGJR*	*NRLLvsTRLL*	*NGJRvsEGC*
Coinbase	0.53	**-3.83**	**-6.53**	0.59	**-6.84**	**-3.53**
Bitfinex	0.28	**-3.03**	**-5.37**	0.58	**-7.27**	**-3.95**
Bitstamp	0.51	**-3.49**	**-4.34**	1.22	**-4.13**	-0.66

Table 6: Gaussian lower than Student's t

Table 6 shows the result of comparing MSE of two models, whose names are given in the column header 'TRUE' shows that the left hand side of 'vs' in column header has lower MSE than its right hand side.

	NGCvsTGC	*NGSvsTGS*	*NRLvsTRL*	*NGJRvsTGJR*	*NRLLvsTRLL*	*NGJRvsEGC*
Coinbase	FALSE	TRUE	TRUE	TRUE	TRUE	TRUE
Bitfinex	FALSE	TRUE	TRUE	TRUE	TRUE	TRUE
Bitstamp	FALSE	TRUE	TRUE	TRUE	TRUE	TRUE

Table 5 depicts the fact that Gaussian and Student's t GARCH and GJR-GARCH models are not providing statistically different out-of-sample forecasts in any of the markets. Nevertheless, NGS and TGS exhibit statistically different out-of-sample performance. Additionally, I see from DM test that Student's t distribution provides statistically different forecasts for other models and from

Table 6 that MSE is lower for Gaussian distribution. Moreover, I see that MSE for N-GJR is lower than EGARCH, however, EGC and NGJR are not providing significantly different results. I can argue that Normal distribution shows better out of sample performance compared to Student's t distribution. I repeat the procedure described above for comparison between different models with Normal distribution. Results of this step are presented in Table 7 and Table 8.

Table 7: DM test for Normal models

Table 7 shows DM test statistic for comparison of different models with Normal distribution. Bolded values show that null hypothesis can be rejected at 5% significance level.

	NGCvsNRL	*NRLvsNRLL*	*NGJRvsNRL*	*NGCvsNGJR*
Coinbase	**-3.27**	**-3.01**	-1.89	-0.61
Bitfinex	**-2.74**	**-3.07**	**-2.69**	**-1.97**
Bitstamp	-1.82	**-3.14**	1.01	-1.66

Table 8: MSE comparison for Normal models

Table 8 depicts the result of comparing MSE of different models with Normal distribution. 'TRUE' shows that the left hand side of 'vs' in column header has lower MSE than its right hand side.

	NGCvsNRL	*NRLvsNRLL*	*NGJRvsNRL*	*NGCvsNGJR*
Coinbase	TRUE	TRUE	TRUE	TRUE
Bitfinex	TRUE	TRUE	TRUE	TRUE
Bitstamp	TRUE	TRUE	FALSE	TRUE

From Table 8, I see that Normal GARCH has the lowest MSE among all models. Moreover, Normal GJR has lower MSE than Normal Realized GARCH model, which in turn has lower MSE than Normal Realized GARCH with leverage.

The null hypothesis can be rejected for all comparisons for Bitfinex, but for Bitstamp, the null can be rejected only for comparison between NRL and NRLL, while for Coinbase, it can be refuted for comparisons between NGC and NRL, and NRL and NRLL. Overall, results show that statistically different out of sample performance depends not only on the models being compared, but also on the market in which the comparison is being performed.

In general, it can be concluded that simple Normal GARCH, which is equivalent to Normal GAS, has the best out of sample performance. This result is in stark contrast with in-sample performance results. Obviously, this difference can also be due to specific characteristics of time series in the period under study. Such characteristics can include sudden jumps in volatility or observations from tails of distribution.

5.2 Multivariate Models

In this section, the results of Multivariate GAS models are presented. Table 9 shows the result of equi-correlation model for Gaussian and Student's t distributions. I can see from results of equi-correlation model that the estimated value of ρ is 0.99, and number of degrees of freedom ν for Student's t is equal to 3.16. Therefore, taking ρ and ν into account, I argue that the markets are highly correlated and returns are drawn from a fat tailed distribution.

Table 9: Equi Correlation Estimation

Table 9 provides the result of estimating Equi-Correlation structure. Bolded values highlight the model with better in sample performance.

	ρ	ν	*LL*	*AIC*	*BIC*
Normal-Equi	0.99		8,275.27	-16,506.53	-16,401.38
t-Equi	0.99	3.16	**8,802.32**	**-17,558.63**	**-17,448.70**

Table 10 and Table 11 depict estimation results of matrices A and B for equi-correlation structure. In each table, I provide estimated matrices for both Normal and Student's t densities.

Table 10: Matrix A for equi-correlation structures

Table 10 shows the estimation of matrix A for equi-correlation structure of multivariate GAS model. Left panel shows the estimation result for Normal distribution and right panel depicts the result for Student's t distribution assumption.

		Coinbase	**Bitfinex**	**Bitstamp**
Normal	**Coinbase**	-0.13	0.14	0.13
	Bitfinex	-0.05	0.17	0
	Bitstamp	-0.08	0.09	0.12

		Coinbase	**Bitfinex**	**Bitstamp**
Student's t	**Coinbase**	0.1	0.01	9.24E-04
	Bitfinex	5.23E-05	0.06	0.05
	Bitstamp	-1.18E-03	0.08	0.03

Table 11: Matrix B for equi-correlation structures

Table 11 exhibits estimation results of Matrix B for equi-correlation structure of multivariate GAS model. Left panel shows the estimation results for Normal distribution, and right panel provides the result for student's t distribution assumption.

		Coinbase	**Bitfinex**	**Bitstamp**
Normal	**Coinbase**	0.95	-8.49E-05	-0.05
	Bitfinex	-0.11	0.99	0.03
	Bitstamp	0.01	-0.02	0.92

		Coinbase	**Bitfinex**	**Bitstamp**
Student's t	**Coinbase**	0.98	0.01	-1.06E-05
	Bitfinex	1.24E-04	0.99	3.99E-03
	Bitstamp	-8.08E-04	-1.65E-03	0.99

As expected for B matrices, I have diagonal elements approximately equal to one, and elements close to zero for other elements in both Student's t and Gaussian distribution. Moreover, for matrices A, I have diagonal elements which are lower than diagonal elements of matrix B.

First diagonal element of Matrix A for equi-correlation structure with Normal distribution is negative. This negative value indicates that information conveyed from Coinbase is not the most relevant to predict its next day's volatility, but it is the information provided by the other two markets that provides relevant information for predicting next day volatility of Coinbase.

Also, the estimated elements on first row of Matrix A for Normal distribution are very close in absolute value, and the estimated correlation between markets is very close 1. These results exhibit probable existence of factor structure between volatility of Bitcoin in different markets, however, due to time constraint, I did not investigate this.

Table 12 illustrates the results of estimating constant correlation, which with multivariate GAS model. In Table 12, ConstRN refers to multivariate GAS with constant correlation and Normal distribution and ConstRt refers to multivariate GAS with constant correlation and Student's t density. These models include one correlation estimate between each two markets. Table 13 and Table 14 exhibit estimated correlation matrix for different distributions.

Table 12: Constant Correlation Estimation

Table 12 depicts results of estimating constant correlation model for both distributions. Bolded values highlight the model with better in sample performance. Diagonal elements of matrices A and B are given in the table as well.

	a_1	a_2	a_3	a_4	b_1	b_2	b_3	b_4	ν	*LL*	*AIC*	*BIC*
ConstRN	0.07	0.07	0.07	0.03	0.96	0.96	0.96	0.82		8,357.77	-16,687.54	-16,620.62
ConstRt	0.11	0.1	0.1	0.21	0.97	0.98	0.97	0.39	3.31	**8,813.95**	**-17,597.90**	**-17,526.21**

Table 13: Correlation matrix - Normal constant correlation

Table 13 shows the estimated correlation matrix for constant correlation model with Normal distribution.

	Coinbase	*Bitfinex*	*Bitstamp*
Coinbase	1	0.99	0.99
Bitfinex	0.99	1	0.99
Bitstamp	0.99	0.99	1

Table 14: Correlation matrix - Student's t constant correlation

Table 14 exhibits the estimated correlation matrix for constant correlation model with Student's t distribution.

	Coinbase	*Bitfinex*	*Bitstamp*
Coinbase	1	0.99	0.99
Bitfinex	0.99	1	1
Bitstamp	0.99	1	1

Results from the constant correlation estimation indicate strong correlation, approximately equal to one, for the markets and heavy tail distribution with degrees of freedom ν equal to 3.31. Again I observe that elements of matrix B which is diagonal in this specification are close to 1, and diagonal elements of matrix A are close to zero. Comparison in terms of AIC and BIC criterion lead us to conclude that Student's t distribution provides more appropriate predictions in both types of models. Moreover, constant correlations provide lower AIC and BIC criterion than equi-correlation specification.

In order to represent, predictions of Multivariate model for constant correlation structure, I provided Figure 8, which depicts comparison of predictions for Student's t and Gaussian densities. I can obviously see that Student's t specification allows for realizations of tails and does not include spikes at certain points. Similar plot is provided for equi-correlation structure.

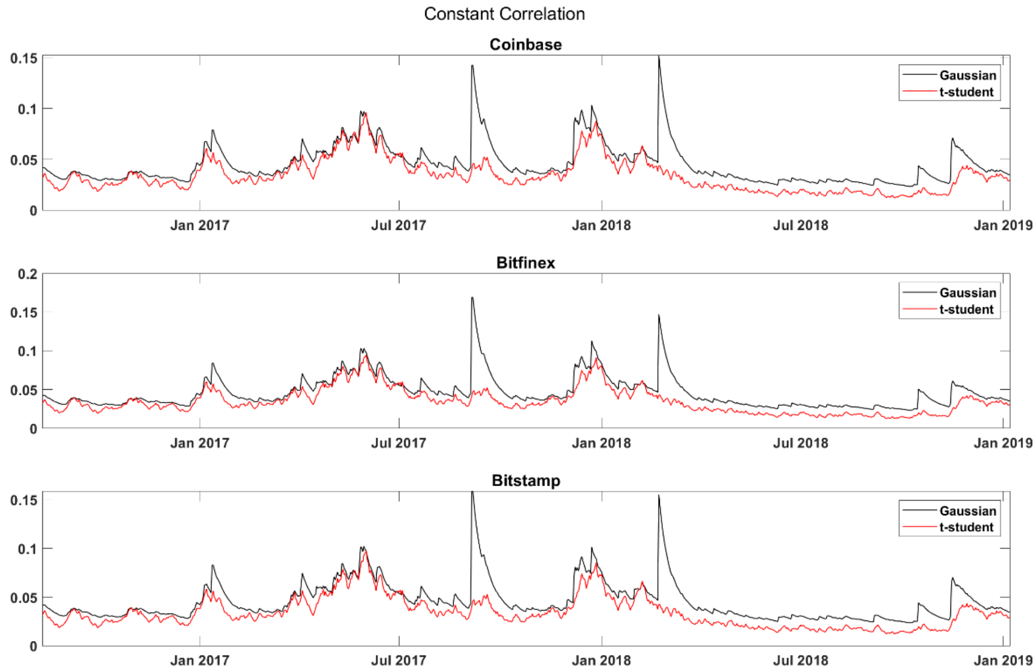

Figure 8: Comparison of Student's t and Gaussian predictions for constant correlation model

Figure 8 depicts forecasted volatilities of all the markets for multivariate GAS with constant correlation model and Student's t and Normal distributions. This figure shows absorption of outliers and observations from tails for Student's t distribution.

6. Simulation Study

In this section, I briefly investigate behavior of models used in this study in a simulation setting. In order to prepare the data set, I generated a bivariate set of variables with constant correlation, set equal to 0.2, and t-student distribution. Following equation provides the equation for volatility of the data generated:

$$\sigma_{1t} = 1 \;\; , \mathrm{t} \in (1{,}1000) \;\; ; \;\; \sigma_{1t} = 5 \;\; , \mathrm{t} \in (1001, 2000)$$

$$\sigma_{2t} = 7 + 5\sin\left(\frac{2\pi t}{400}\right)$$

Volatility path of one of the generated variables follows a process with structural break, and the volatility path of the other variable follows a sine wave process. Generated data set includes 2000 return, and the degrees of freedom is equal to 3, which provides basis for depicting difference of t-GAS. Figure 9 shows summary of simulated data with Student's t distribution.

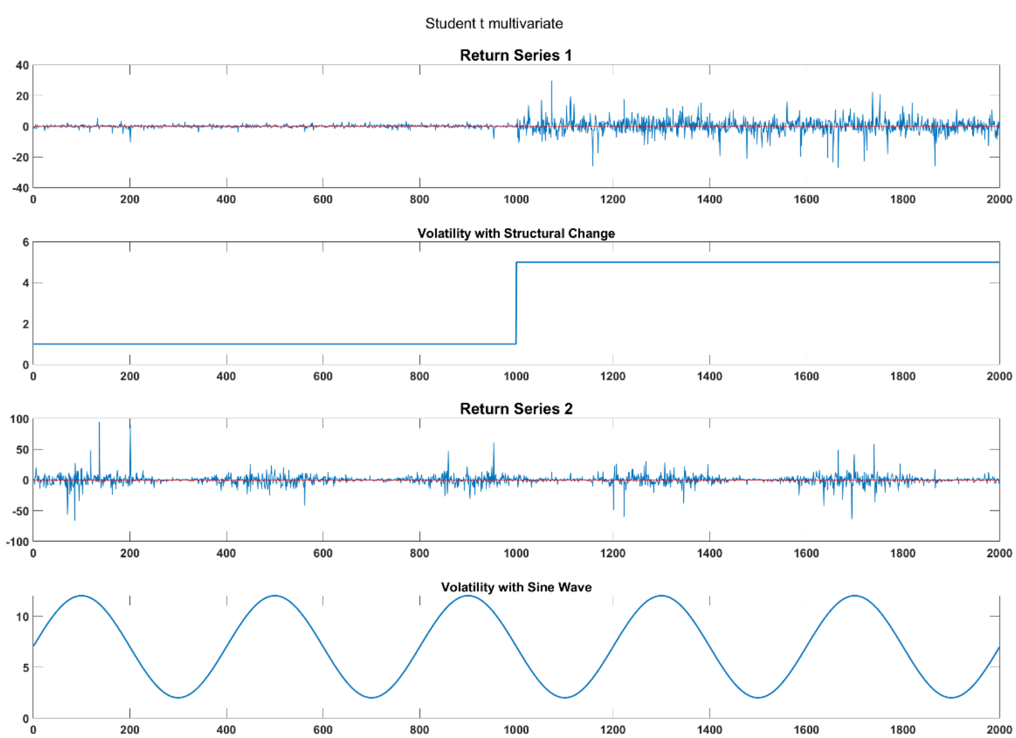

Figure 9: Simulated Data with Student's t distribution
Figure 9 displays the summary of generated data set for simulation study. Panels 1 and 3 show the return series, and panels 2 and 4 depic the volatility path used to generate data set.

Since generated data set does not include realized measure, I will not estimate those models. Moreover, I will only estimate GJR-GARCH model with Normal and Student's t distributions among leverage models, and I exclude EGARCH since I included it only with Normal distribution. Figure 10 displays the result of estimating GARCH and GAS models for simulated data with sine wave for volatility.

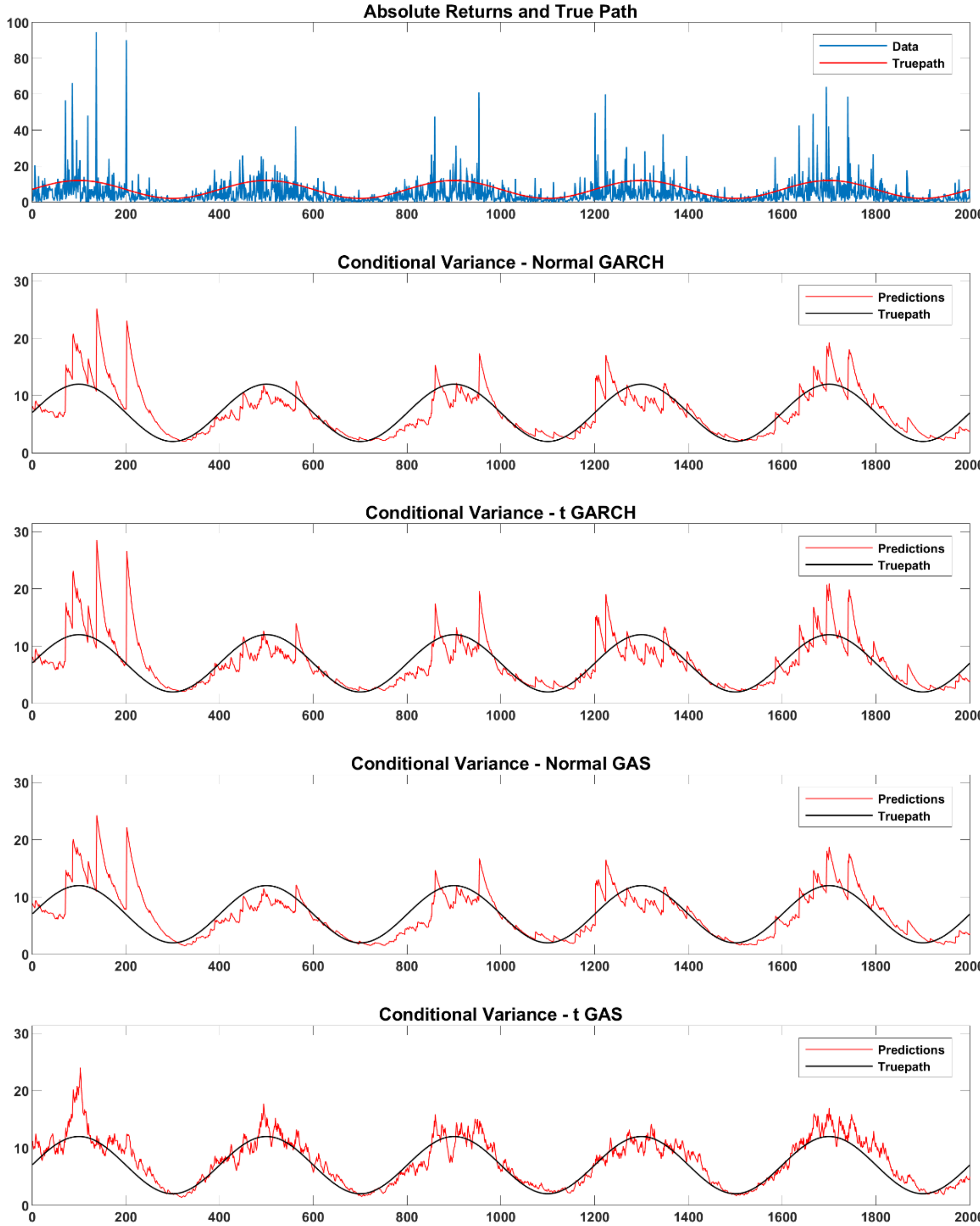

Figure 10: GARCH and GAS results for simulation study

Figure 10 exhibits predictions of different densities for GARCH and GAS models. In addition, I provide the data generating process for comparing with predictions of different models. Panel 1 shows the absolute return and volatility path used to generate returns. Panels 2 and 3 depict forecasts of GARCH with Normal and Student's t densities around the volatility path used to generate data set. Panels 4 and 5 exhibit variability of GAS model with Normal and Student's t distribution around the volatility path utilized to simulate data.

Figure 11 shows the result of estimating GJR model with different distributions. It is worth mentioning that all the models show the ability of tracking true path, and can provide forecasts close to data generating process.

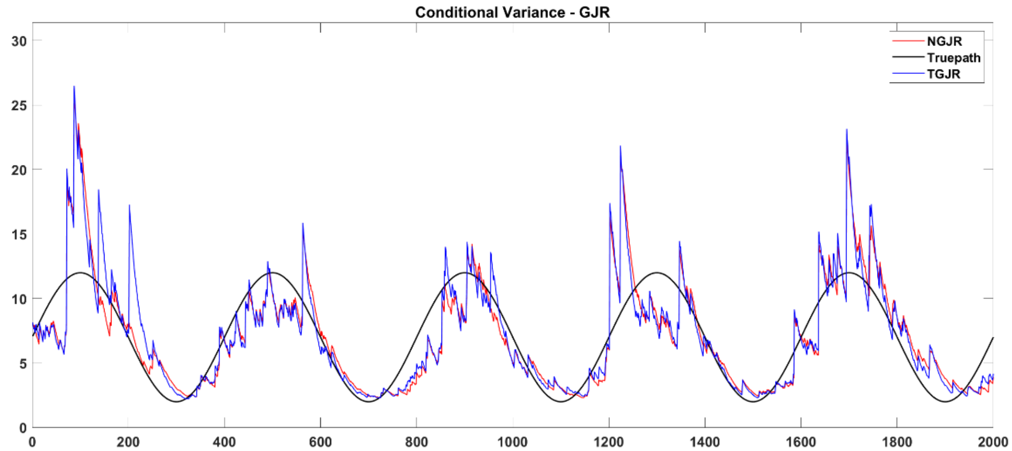

Figure 11: GJR models for simulated data
Figure 11 shows the predictions of Normal GJR and Student's t GJR models, and the data generating process.

From Figure 11 I can see that Normal and Student's t GJR models are providing very close predictions. This is due to close estimations of parameters in the model, a fact which will be shown in **Error! Reference source not found.**. Moreover, I provide comparison of GARCH and t-GAS models in Figure 12.

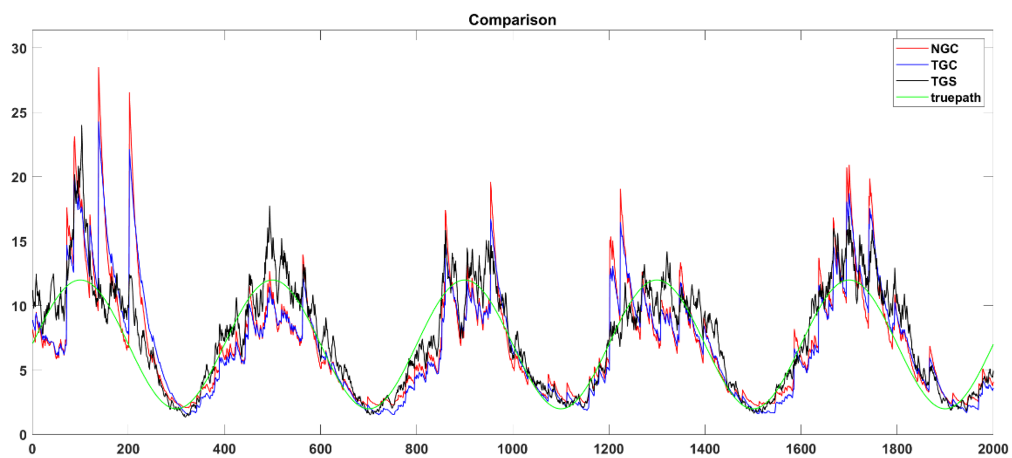

Figure 12: Comparison of GARCH and GAS for simulated data
Figure 12 shows the predictions generated by Normal and Student's t GARCH and predictions given by t-GAS. This figure provides the basis to compare the predictions of these models.

From Figure 12, I can observe that t-GAS needs more observations to adjust the level of predictions. Indeed, this observation is one of the important characteristics of GAS model which allows for observations from heavy tails of distribution. Additionally, predictions generated by t-GAS are smoother compared to those of GARCH models. Table 15 represents results of estimating univariate models for generated data set with sine wave as the volatility.

Table 15: Results of univariate estimation for generated data set

Table 15 depicts the result of estimating univariate models for generate data set. Bolded value emphasize the minimum AIC and BIC among the models.

Model	ω	α	β	α^{-}	ν_1	LL	AIC	BIC
NGC	0.14	0.06	0.94			-3.29	6.58	6.59
NGS	0.00	0.05	1.00			-3.30	6.61	6.62
TGC	0.26	0.08	0.92		2.92	-3.05	6.10	6.12
TGS	1.98E-04	0.07	1.00		2.63	**-3.03**	**6.06**	**6.07**
NGJR	0.17	0	0.95	0.09		-3.27	6.55	6.56
TGJR	0.25	0.03	0.93	0.08	2.91	-3.05	6.10	6.11

As I can see in Table 15 minimum AIC and BIC are observed for t-GAS. In addition, degrees of freedom for models with Student’s t distribution are close to degrees of freedom used to generate data set. In the next step, I will provide results of estimating multivariate models. First I will estimate equi-correlation structure and provide the subplots in Figure 13.

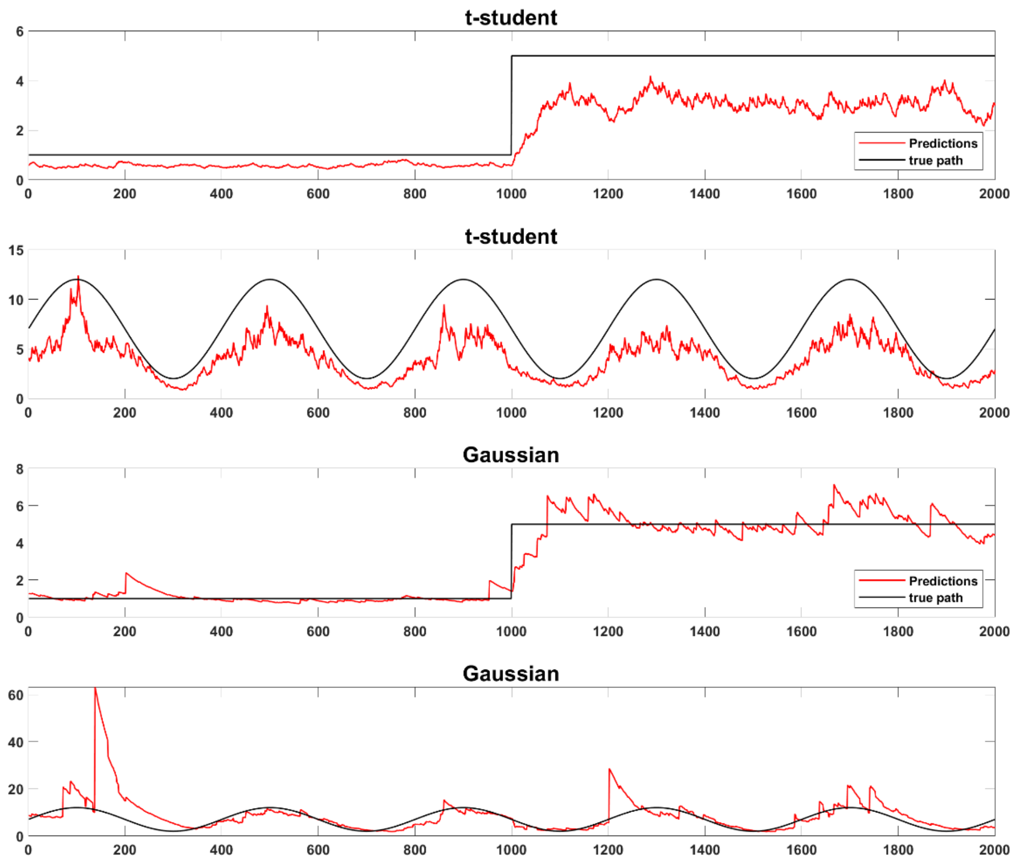

Figure 13: Equi-correlation for simulated data

Figure 13 depicts comparison of predictions generated by equi-correlation model with Normal and Student's t distributions. In addition, the volatility path used to generate the data set is given for comparison with predictions. Panels 1 and 2 show the forecasts with Student's t distribution, and panels 3 and 4 depict the predictions with Normal distribution.

I can clearly see a characteristic of t-GAS model which is smoothly updating to new levels by comparing the panels related to the series with structural break. In addition, I can see in the panel related to series with sine wave that t-GAS is relatively smoother and does not contain spikes. I also provide the results of estimating multivariate GAS model with constant correlation structure in Figure 14, in which I have similar observation.

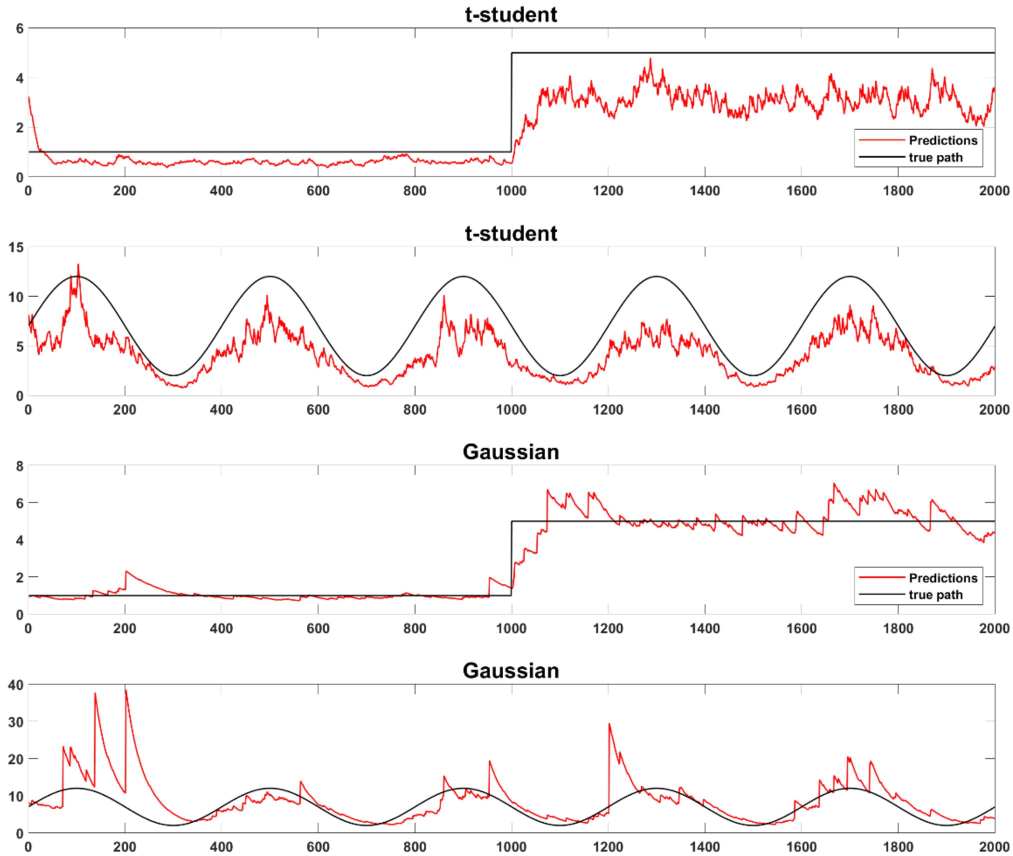

Figure 14: Constant correlation for simulated data

Figure 14 shows the predictions of constant correlation model with different densities. In addition, I present the volatility path used to generate data set for comparison. Panels 1 and 2 show the forecasts with Student's t distribution, and panels 3 and 4 depict the predictions with Normal distribution.

In Table 16 and Table 17, I present estimation results of matrices A and B for simulated data set. In these tables, SB refers to data with Structural Break, and SW refers to data with Sine Wave. I can see that diagonal elements of matrix B for Gaussian and Student's t distributions are close to one, and that those of matrix A for both distributions are close to zero. Moreover, off diagonal elements in both matrices are close to zero.

Table 16: Matrix A of equi-correlation specification

Table 16 shows the A matrices, which are estimated through equi-correlation structure, for simulated data.

		SB	SW			SB	SW
Normal	**SB**	0.02	0.00	**Student's t**	**SB**	0.04	-0.01
	SW	-0.02	0.04		**SW**	-0.01	0.07

Table 17: Matrix B of equi-correlation specification

Table 17 provides the B matrices, which are estimated through equi-correlation structure, for simulated data.

		SB	SW			SB	SW
Normal	**SB**	1.00	0.00	**Student's t**	**SB**	1.00	0.00
	SW	0.00	1.00		**SW**	0.00	0.99

In Table 18, I provide the result of estimation for equi-correlation specification. As I can see, estimated values of correlation for Normal and Student's t are not similar. For Student's t distribution I have correlation equal to 0.16, and for Normal distribution I have correlation equal to 0.01. It must be mentioned that correlation used to generate the data set is 0.2. Moreover, the number of degrees of freedom in Student's t specification is 2.65 rather than 3 which was used to create the data set. AIC and BIC show that for equi-correlation structure multivariate GAS model with Student's t distribution has better in sample performance than Normal distribution.

Table 18: Result of equi-correlation specification for simulated data

Table 18 show the correlation, likelihood, AIC and BIC for equi-correlation structure. Bolded values show the model with better in sample performance.

	ρ	ν	*LL*	*AIC*	*BIC*
Normal-Equi	0.01		-11178.48	22378.96	22440.57
t-Equi	0.16	2.65	**-10102.15**	**20228.30**	**20295.51**

In Table 19, the result of constant correlation model is provided. I can see that parameters related to logarithm of conditional variance which are given by b_1 and b_2, are approximately equal to one, whereas a parameters which are related to matrix A are close to zero. Moreover, I estimate number of degrees of freedom for Student's t specification is 2.63, and correlation is estimated to be 0.16. In addition, for Gaussian specification correlation value is estimated to be -0.06.

Table 19: Result of constant correlation model for simulated data

Table 19 provides the result of estimating constant correlation model for the simulated data set. Bolded values emphasize the model with better in sample performance.

	a_1	a_2	a_3	b_1	b_2	b_3	ν	ρ	LL	AIC	BIC
ConstRN	0.02	0.04	0.05	1.00	1.00	0.9		-0.06	-11220.85	22459.70	22510.10
ConstRt	0.06	0.08	0.05	1.00	1.00	0.9	2.63	0.16	**-10126.46**	**20272.91**	**20328.92**

Estimations above show that Student's t specification performs better in terms of converging to true correlation parameter for both equi-correlation and constant correlation specifications.

7. Conclusion

Considering in sample results provided by AIC and BIC, I conclude that among GARCH and GAS models, which do not include leverage, t-GAS outperforms other models for modelling volatility of Bitcoin in all the exchanges. This finding was expected, because t-GAS uses efficient update and allows for observations of outliers or realizations from tails of distribution. In addition, plots provided, in the body and appendix, display smoother paths for predictions given by t-GAS, an observation closely related to efficient filter.

Among models including leverage, but excluding realized measures, t-GJR model outperforms the other models. Moreover, among models containing realized measure, Realized GARCH model with leverage function and Student's t distribution performs better in terms of AIC and BIC.

However, out-of-sample performance of models shows that Normal GARCH (equivalent to Normal GAS) has the best performance among all the models. This result can be due to sudden shocks in the window of performing out-of-sample analysis.

In multivariate part, I observe that correlations among markets are estimated to be approximately one. This observation shows us that volatility in markets generally moves in the same direction. Moreover, Student's t density assumption provides lower AIC and BIC in each of the multivariate specifications, which are equi-correlation and constant correlation. In addition, constant correlation provides lower AIC and BIC than equi-correlation structure.

Plots given in this study depict an important characteristic of t-GAS model. This model can absorb outliers, and observations from tails, additionally discounting information from such realizations. Moreover, t-GAS provides smoother path compared to that of GARCH or t-GARCH. Moreover, in multivariate case, it is shown that Student's t distribution for t-GAS absorbs shocks compared to Gaussian density for the same model.

8. References

Aalborg, H. A., Molnár, P. & de Vries, J. E., 2019. What can explain the price, volatility and trading volume of Bitcoin?. *Finance Research Letters,* Issue 29, pp. 255-265.

Andersen, T. G. & Bollerslev, T., 1998. Deutsche mark-dollar volatility: Intraday activity patterns, macroeconomic announcements, and longer run dependencies. *Journal of Finance,* 53(1), pp. 219-265.

Andersen, T. G., Bollerslev, T., Diebold, F. X. & Labys, P., 1999. Realized volatility and correlation. *LN Stern School of Finance Department Working Paper,* Volume 24.

Andersen, T. G., Bollerslev, T., Diebold, F. X. & Labys, P., 2003. Modeling and forecasting realized volatility. *Econometrica,* 71(2), pp. 579-625.

Baba, Y., Engle, R. F., Kraft, D. F. & Kroner, K. F., 1990. *Multivariate simultaneous generalized ARCH,* s.l.: Manuscript, University of California, San Diego, Department of Economics.

Bariviera, A. F., José Basgall, M., Hasperué, W. & Naiouf, M., 2017. Some stylized facts of the Bitcoin market. *Physica A.*

Baur, D. G. & Dimpfl, T., 2018. Asymmetric volatility in cryptocurrencies Predicting Financial Markets with Google Trends Data View project Asymmetric Volatility in Cryptocurrencies. *Elsevier.*

Beneki, C., Koulis, A., Kyriazis, N. A. & Papadamou, S., 2019. Investigating volatility transmission and hedging properties between Bitcoin and Ethereum. *Research in International Business and Finance,* Volume 48, pp. 219-227.

Blasques, F., Koopman, S. J. & Lucas, A., 2015. Information-theoretic optimality of observation-driven time series models for continuous responses. *Biometrika,* 102(2), pp. 325-343.

Bollerslev, T., 1986. Generalized autoregressive conditional heteroskedasticity. *Journal of econometric,* pp. 307-327.

Bollerslev, T., 1990. Modelling the coherence in short-run nominal exchange rates: a multivariate generalized ARCH model. *The review of economics and statistics,* pp. 498-505.

Bollerslev, T., Engle, R. F. & Wooldridge, J. M., 1988. A capital asset pricing model with time-varying covariances. *Journal of political Economy,* 96(1), pp. 116-131.

Bouri, E., Azzi, G. & Dyhrberg, A. H., 2016. On the return-volatility relationship in the Bitcoin market around the price crash of 2013. *Available at SSRN 2869855.*

Brandvold, M., Molnár, P., …, K. V. -. …. o. I. F. & 2015, u., n.d. Price discovery on Bitcoin exchanges. *Elsevier.*

References

Brandvold, M., Peter, M., Kristian, V. & Ole Christian, A. V., 2015. Price discovery on Bitcoin exchanges. *Journal of International Financial Markets, Institutions and Money,* pp. 18-35.

Budish, E., 2018. *The Economic Limits of Bitcoin and the Blockchain,* s.l.: s.n.

Conrad, C., Custovic, A. & Ghysels, E., 2018. Long-and short-term cryptocurrency volatility components: A GARCH-MIDAS analysis. *Journal of Risk and Financial Management,* 11(2), p. 23.

Corsi, F., 2009. A simple approximate long-memory model of realized volatility. *Journal of Financial Econometrics,* 2(7), pp. 174-196.

Creal, D., Jan Koopman, S., Lucas, A. & Jan KOOPMAN, S., 2012. A Dynamic Multivariate Heavy-Tailed Model for Time-Varying Volatilities and Correlations. *amstat.tandfonline.com,* 10, 29(4), pp. 552-563.

Creal, D., Koopman, S. J. & Lucas, A., 2013. Generalized autoregressive score models with applications. *Journal of Applied Econometrics,* 28(5), pp. 777-795.

Crosby, M., Pradan, P., Sanjeev, V. & Vignesh, K., 2016. Blockchain technology: Beyond bitcoin. *Applied Innovation,* 2(6-10), p. 71.

Diebold, F. X. & Mariano, R. S., 1995. Comparing forecast accuracy. *Journal of Business and.*

econometrics, T. B. -. J. o. & 1986, u., n.d. Generalized autoregressive conditional heteroskedasticity. *u.arizona.edu.*

Engle, R., 2002. Dynamic conditional correlation: A simple class of multivariate generalized autoregressive conditional heteroskedasticity models. *Journal of Business & Economic Statistics,* 20(3), pp. 339-350.

Engle, R. F., 1982. Autoregressive conditional heteroscedasticity with estimates of the variance of United Kingdom inflation. *Econometrica: Journal of the Econometric Society,* pp. 987-1007.

Engle, R., Ghysels , E. & Sohn, B., 2013. Stock Market Volatility and Macroeconomic Fundamentals. *The Review of Economics and Statistics,* 95(3), pp. 776-797.

Fang, L., Bouri, E., Gupta, R. & Roubaud, D., 2019. Does global economic uncertainty matter for the volatility and hedging effectiveness of Bitcoin?. *International Review of Financial Analysis,* Volume 61, pp. 29-36.

Glosten, L. R., Jagannathan, R. & Runkle., D. E., 1993. On the relation between the expected value and the volatility of the nominal excess return on stocks. *The journal of finance,* pp. 1779-1801.

Godsiff, P., 2015. *Bitcoin: Bubble or blockchain.* s.l., Springer Science and Business Media Deutschland GmbH, pp. 191-203.

Griffin, J. M. & Shams, A., 2019. Is bitcoin really un-tethered?. *Available at SSRN 3195066.*

Hansen, P. R., Huang, Z. & Shek, H. H., 2012. Realized GARCH: a joint model for returns and realized measures of volatility. *Journal of Applied Econometrics,* 27(6), pp. 877-906.

Heilman, E., Foteini, B. & Sharon, G., 2016. *Blindly signed contracts: Anonymous on-blockchain and off-blockchain bitcoin transactions.* Berlin, Heidelberg, Springer, pp. 43-60.

Katsiampa, P., 2017. Volatility estimation for Bitcoin: A comparison of GARCH models. *Economics Letters,* Issue 158, pp. 3-6.

Katsiampa, P., 2019. Volatility co-movement between Bitcoin and Ether. *Finance Research Letters,* Volume 30, pp. 221-227.

Klein, T., Thu, H. P. & Walther, T., 2018. Bitcoin is not the New Gold–A comparison of volatility, correlation, and portfolio performance. *International Review of Financial Analysis,* Volume 59, pp. 105-116.

Koopman, S. J., Lucas, A. & Zamojski, M., 2017. *Dynamic term structure models with score-driven time-varying parameters: estimation and forecasting.* s.l.:Economic Institute.

Letters, A. U. -. E. & 2016, u., n.d. The inefficiency of Bitcoin. *Elsevier.*

Letters, P. K. -. E. & 2017, u., n.d. Volatility estimation for Bitcoin: A comparison of GARCH models. *Elsevier.*

Makarov, I. & Antoinette, S., 2020. Trading and arbitrage in cryptocurrency markets. *Journal of Financial Economics,* 135(2), pp. 293-319.

Meiklejohn, S. et al., 2013. *A fistful of bitcoins: characterizing payments among men with no names.* s.l., In Proceedings of the 2013 conference on Internet measurement conference.

Nakamoto, S. & Bitcoin, A., 2008. *A peer-to-peer electronic cash system. Bitcoin.* [Online] Available at: https://bitcoin. org/bitcoin. pdf

Nelson, D. B., 1991. "Conditional heteroskedasticity in asset returns: A new approach." (1991): 347-370.. *Econometrica: Journal of the Econometric Society,* pp. 347-370.

Ølnes, S., 2016. *Beyond bitcoin enabling smart government using blockchain technology.* Cham, Springer.

Ron, D. & Adi, S., 2013. *Quantitative analysis of the full bitcoin transaction graph.* Berlin, Heidelberg, In International Conference on Financial Cryptography and Data Security, pp. 6-24. Springer.

Ruffing, T., Pedro, M.-S. & Aniket, K., 2014. *Coinshuffle: Practical decentralized coin mixing for bitcoin.* Cham, Springer, pp. 345-364.

Scaillet, O., Treccani, A. & Trevisan, C., 2017. *High-Frequency Jump Analysis of the Bitcoin Market,* s.l.: s.n.

Selgin, G., 2015. Synthetic commodity money. *Journal of Financial Stability,* pp. 92-99.

Shephard, N., 2005. *Stochastic volatility: selected readings.* s.l.:Oxford University Press on Demand.

Society, D. N. -. E. J. o. t. E. & 1991, u., n.d. Conditional heteroskedasticity in asset returns: A new approach. *JSTOR.*

Society, R. E. -. E. J. o. t. E. & 1982, u., n.d. Autoregressive conditional heteroscedasticity with estimates of the variance of United Kingdom inflation. *JSTOR.*

Symitsi, E. & Chalvatzis, K. J., 2018. Return, volatility and shock spillovers of Bitcoin with energy and technology companies. *Economics Letters,* Volume 170, pp. 127-130.

Taylor, S. J., 1982. Financial returns modelled by the product of two stochastic processes-a study of the daily sugar prices 1961-75. *Time series analysis: theory and practice,* Issue 1, pp. 203-226.

Tsay, R. S., 2005. *Analysis of financial time series.* s.l.:John wiley & sons.

Tse, Y. K. & Tsui, A. K. C., 2002. A multivariate generalized autoregressive conditional heteroscedasticity model with time-varying correlations. *Journal of Business & Economic Statistics,* 20(3), pp. 351-362.

Urquhart, A., 2016. The inefficiency of Bitcoin. *Economics Letters,* pp. 80-82.

Walther, T., Klein, T. & Bouri, E., 2019. Exogenous drivers of bitcoin and cryptocurrency volatility–a mixed data sampling approach to forecasting. *Journal of International Financial Markets, Institutions and Money,* Volume 63, p. 101133.

9. Appendix

A. Equi-correlation model specification

In the equi-correlation structure, f_t is time varying factor which is in $\log\left(daig\left(D_t^2\right)\right)$. Moreover, following (Koopman, et al., 2017) for derivations, I can write:

$$\nabla_t = 0.5\psi_t{}'\left(D_+{}'H_t^{-1} \otimes H_t^{-1} vec\left(\bar{\nu}\, y_t y_t{}' - H_t\right)\right)$$

$$\mathrm{I}_{t|t-1} = \mathrm{E}\left(\nabla_t \nabla_t{}'\right) = \psi_t{}'\left(\Omega + bc'\right)\psi_t$$

Intermediate terms to implement the model are $D_+ = (D_k{}' D_k)^{-1} D_k$, $\psi_t = D_+\left(I_{\mathrm{N}} \oplus D_t R\right) W_{Dt} D_t^2$, $\nu^N = \nu + N$, $\bar{\nu} = \dfrac{\nu^N}{\nu + y_t H_t^{-1} y_t{}'}$, $\tilde{\nu} = \dfrac{\nu^N}{2\left(\nu^N + 2\right)}$, $\Omega = 0.5\tilde{\nu}\left(D_+{}' H_t^{-1} \otimes H_t^{-1} D_+\right)$, $c = \psi_t{}' vec\left(H_t^{-1}\right)$, $b = \left[2\left(\nu^N + 2\right)\right]^{-1} c$ and $\mathrm{I}_{t|t-1} = \psi_t{}'\left(\Omega + bc'\right)\psi_t$. These terms are obviously written for Student's t density.

Nevertheless, for Gaussian distribution from above expressions we will have $\nu^N \to \infty$, $\bar{\nu} \to 1$, $\tilde{\nu} \to 1$ and $b \to 0$. Therefore, in computations I will have some simplifications, and one less parameter, which is ν, to estimate.

B. Univariate Plots

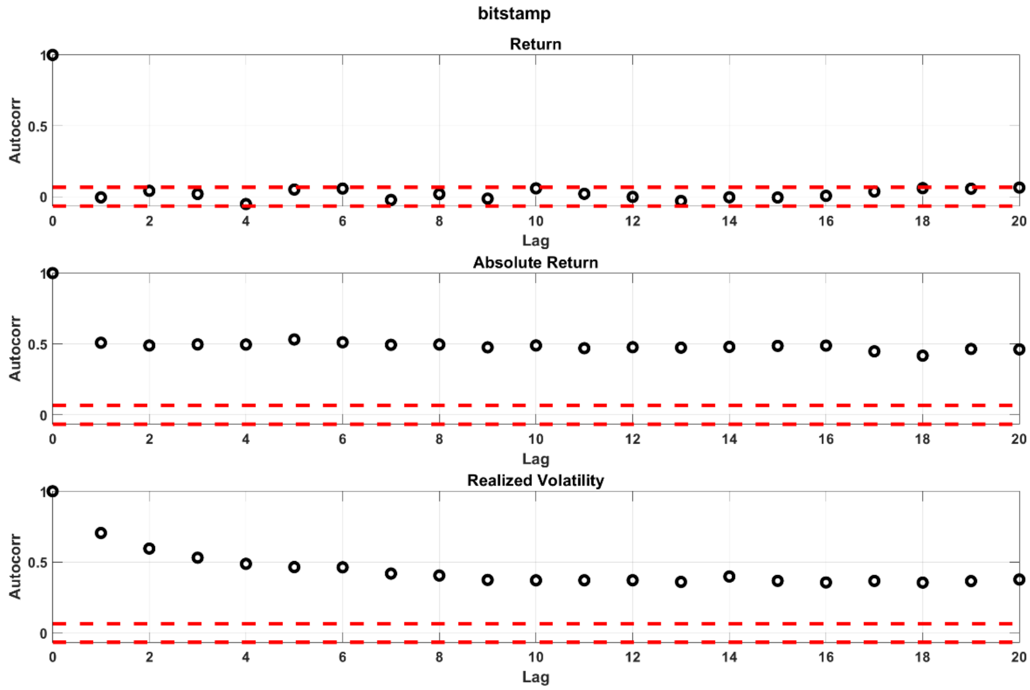

Figure 15: Bitstamp Autocorrelation

Figure 15 shows the autocorrelation results for return, absolute return and realized volatility of Bitstamp. Red dashes show the rejection value of test statistic, and black circles show the estimated statistic. First panel assesses appropriateness of AR process for modelling return, while second and third panels explore suitability of conditional heteroskedasticity models for modelling volatility.

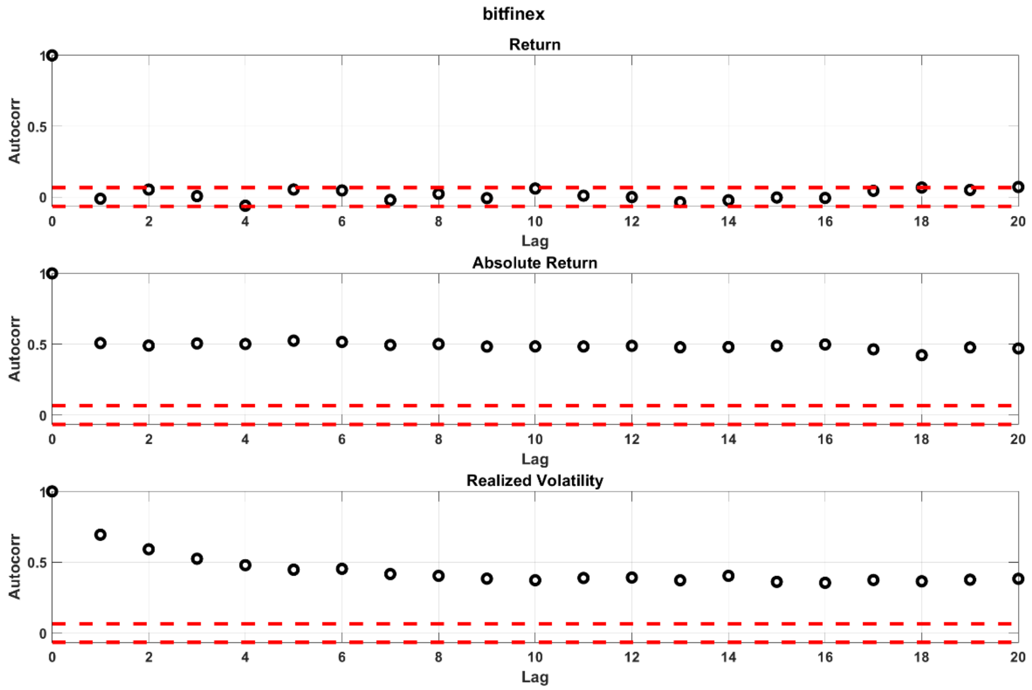

Figure 16: Bitfinex Autocorrelation

Figure 16 shows the autocorrelation results for return, absolute return and realized volatility of Bitfinex. Red dashes show the rejection value of test statistic, and black circles show the estimated statistic. First panel assesses appropriateness of AR process for modelling return, while second and third panels explore suitability of conditional heteroskedasticity models for modelling volatility.

Appendix

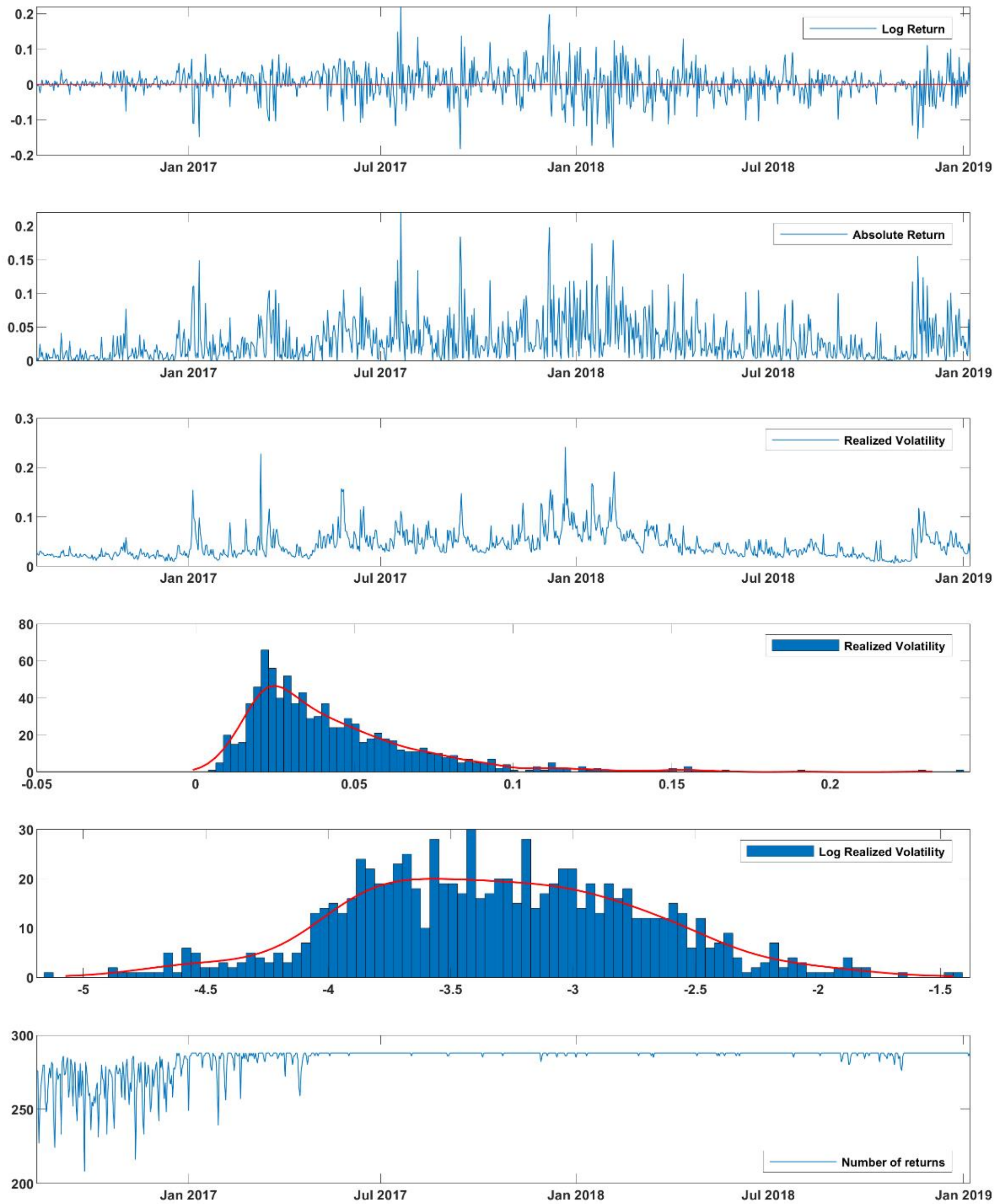

Figure 17: Bitstamp Data Summary

Figure 17 provides visual description of the data of Bitstamp. Return series is depicted in panel 1 in which red line shows zero mean. Panels 2 and 3 depict volatility clustering in the market. Red lines in panels 4 and 5 show the kernel density fitted to realized volatility and log realized volatility. Panel 6 shows the number of observations per day which should be 288 if there is no missing observation.

Appendix

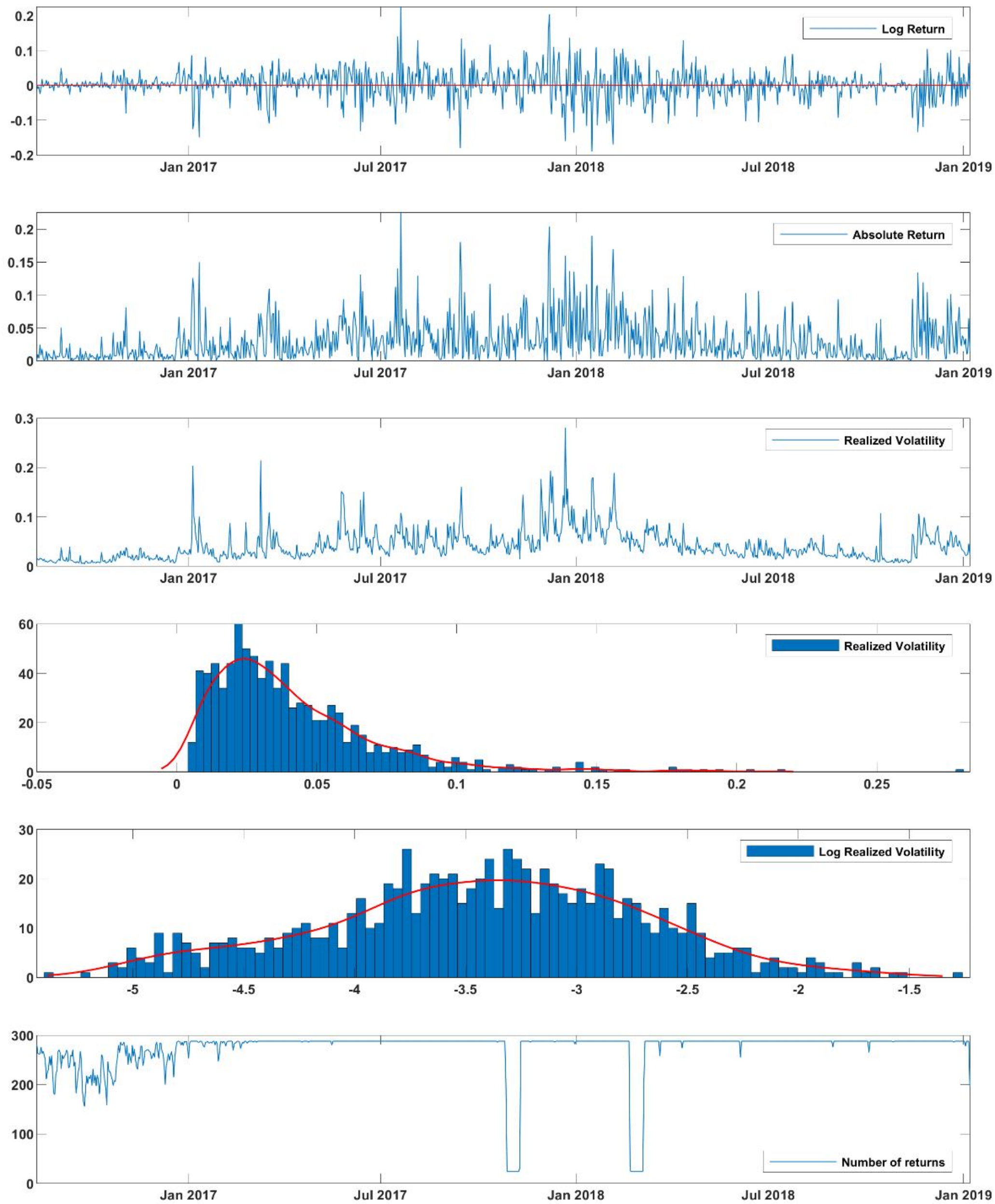

Figure 18: Bitfinex Data Summary

Figure 18 provides visual description of the data of Bitfinex. Return series is depicted in panel 1 in which red line shows zero mean. Panels 2 and 3 depict volatility clustering in the market. Red lines in panels 4 and 5 show the kernel density fitted to realized volatility and log realized volatility. Panel 6 shows the number of observations per day which should be 288 if there is no missing observation.

C. Univariate Plots

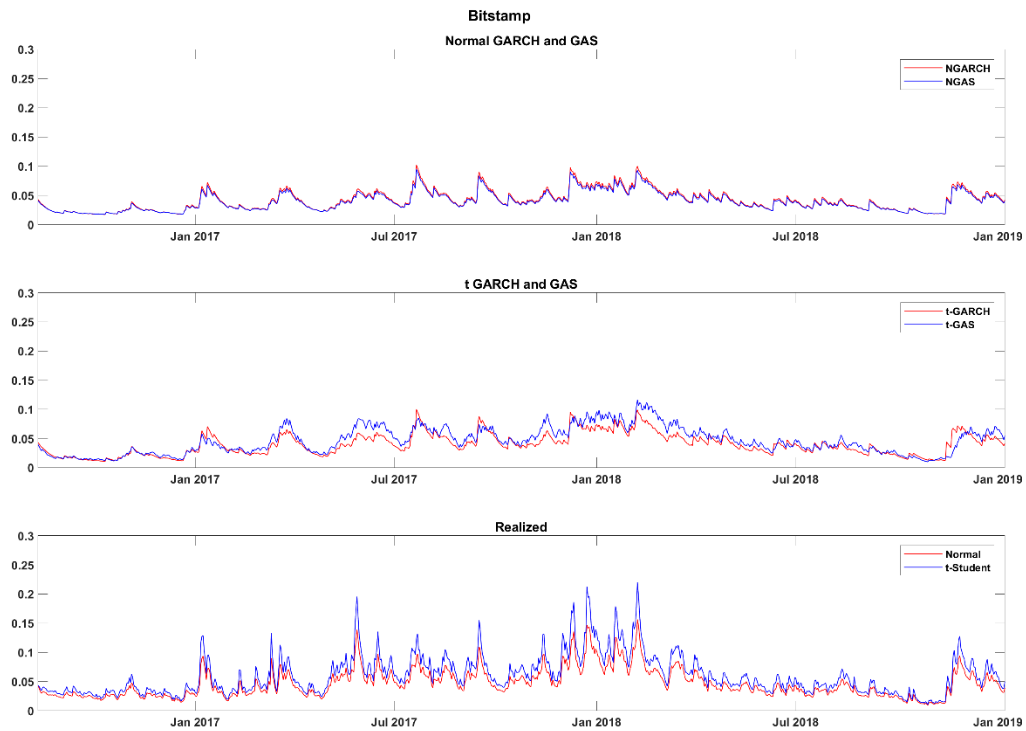

Figure 19: Bitstamp No Leverage comparison

Figure 19 shows the predictions of Normal GARCH and GAS, Student's t GARCH and t-GAS, and Normal and Student's t realized GARCH model and provides the basis for comparing these predictions. First panel shows that Normal GARCH and Normal GAS are essentially the same. However, second panel depicts the difference between GARCH and GAS with Student's t density, and shows that t-GAS has smoother plots, and that spikes occur sooner in GARCH. In addition, while GARCH shows periods of geometric decay, t-GAS does not have similar behavior. Third panel exhibits that Student's t distribution for realized GARCH provides higher prediction in volatility.

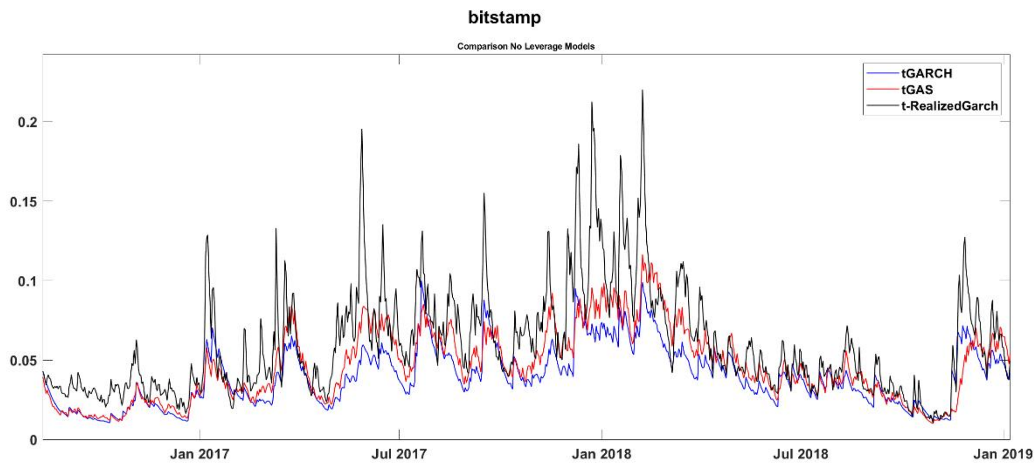

Figure 20: Bitstamp Comparison

Figure 20 shows predictions of different models that do not include leverage and that have student's t distribution. This figure provides the basis for comparison of forecasts between models. Smoother behavior of t-GAS is depicted against both GARCH and Realized GARCH. In addition, spikes happen almost simultaneously in GARCH and realized GARCH while t-GAS needs more observations to shift the level of predictions, and absorbs outlier and observations from tails. Unlike t-GAS, both GARCH and realized GARCH show periods of geometric decay.

Appendix

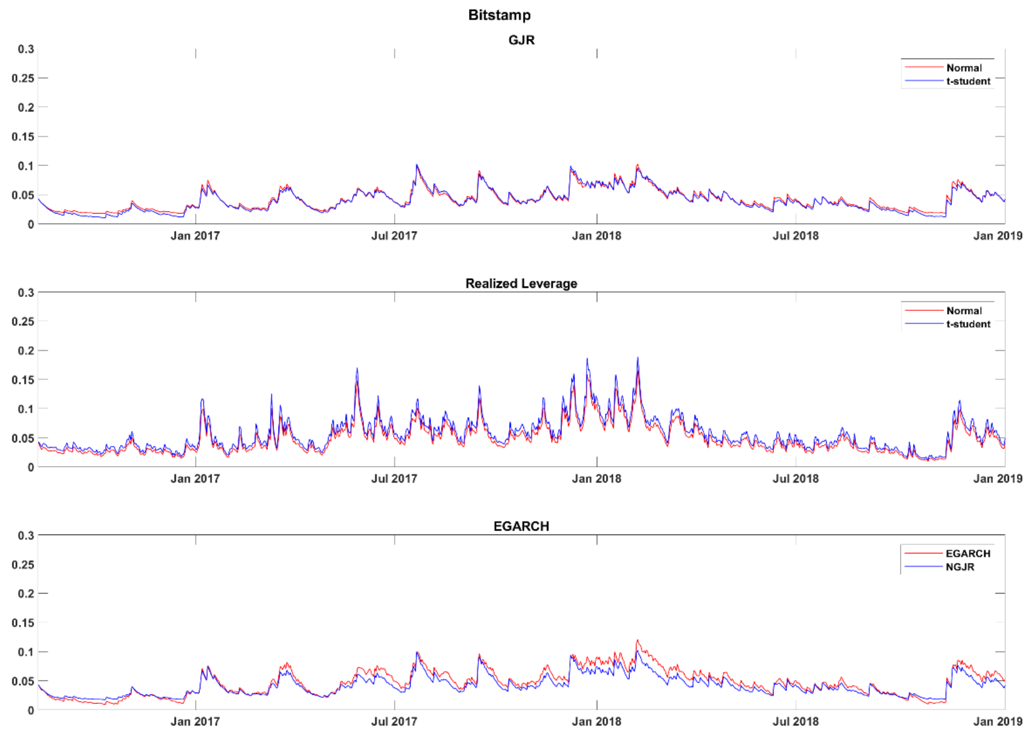

Figure 21: Bitstamp Leverage models

Figure 21 shows the forecasts of models which include leverage function. In panels 1 and 2, I provide results of Normal and student's t GJR and Realized GARCH with Leverage, and in panel 3, I compare the forecasts of EGARCH and Normal GJR model. Normal and Student's GJR models are providing very close predictions, while Student's t Realized with leverage generates higher forecasts than those of the same model with Normal distribution. Third panel shows that EGARCH provides higher predictions than Normal GJR model.

Appendix

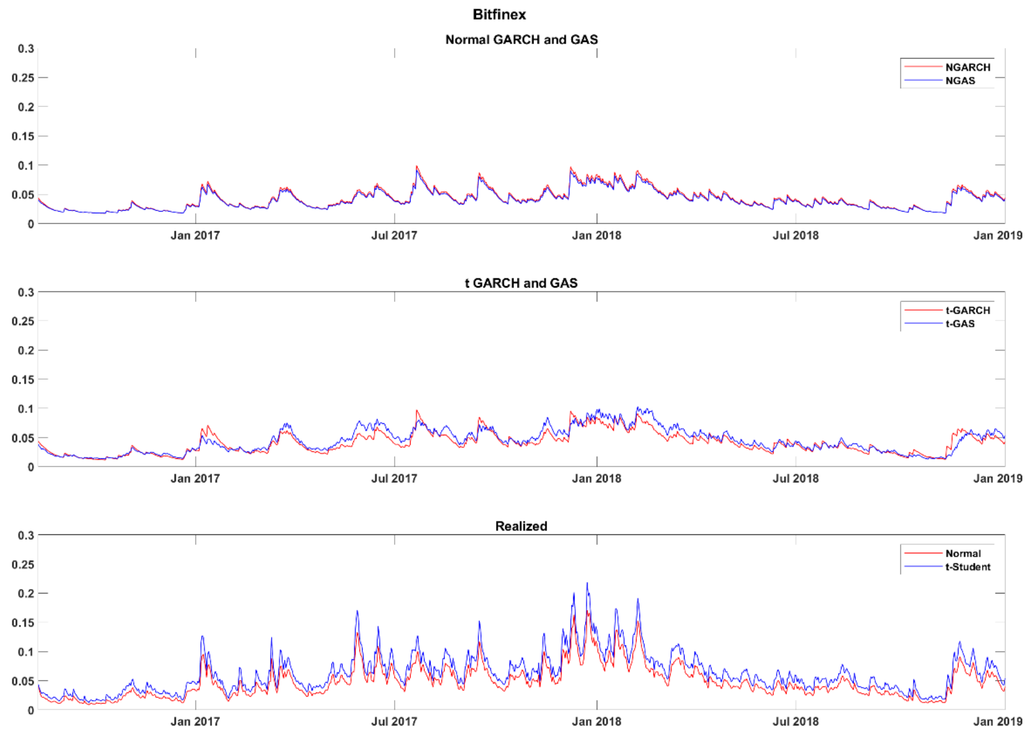

Figure 22: Bitfinex No Leverage

Figure 22 shows the predictions of Normal GARCH and GAS, Student's t GARCH and t-GAS, and Normal and Student's t realized GARCH model and provides the basis for comparing these predictions. First panel shows that Normal GARCH and Normal GAS are essentially the same. However, second panel depicts the difference between GARCH and GAS with Student's t density, and shows that t-GAS has smoother plots, and that spikes occur sooner in GARCH. In addition, while GARCH shows periods of geometric decay, t-GAS does not have similar behavior. Third panel exhibits that Student's t distribution for realized GARCH provides higher prediction in volatility.

Appendix

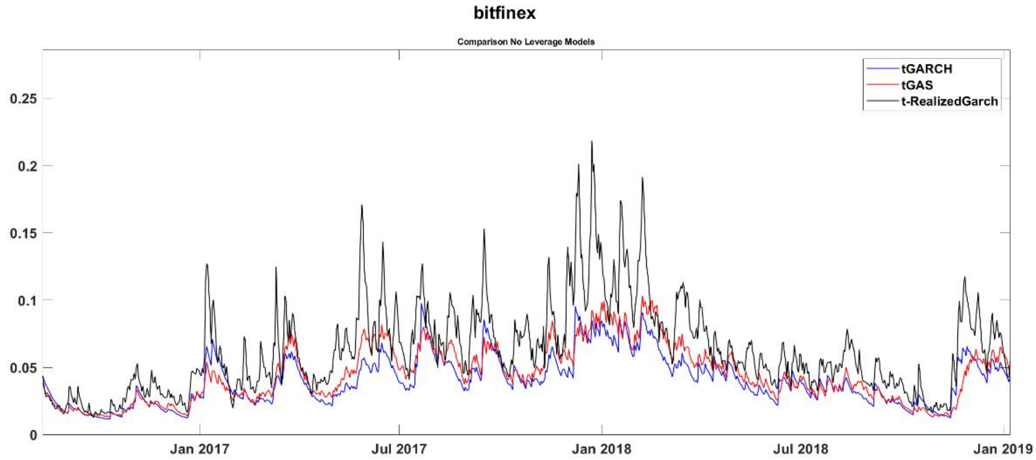

Figure 23: Bitfinex Comparison

Figure 23 shows predictions of different models that do not include leverage and that have student's t distribution. This figure provides the basis for comparison of forecasts between models. Smoother behavior of t-GAS is depicted against both GARCH and Realized GARCH. In addition, spikes happen almost simultaneously in GARCH and realized GARCH while t-GAS needs more observations to shift the level of predictions, and absorbs outlier and observations from tails. Unlike t-GAS, both GARCH and realized GARCH show periods of geometric decay.

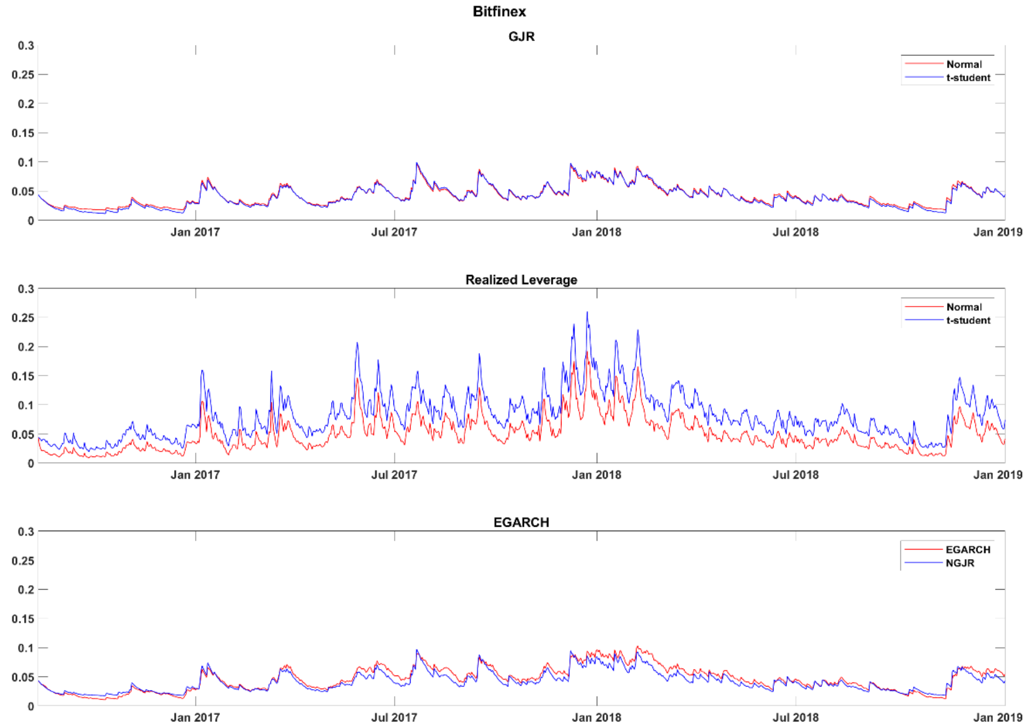

Figure 24: Bitfinex Leverage

Figure 24 shows the forecasts of models which include leverage function. In panels 1 and 2, I provide results of Normal and student's t GJR and Realized GARCH with Leverage, and in panel 3, I compare the forecasts of EGARCH and Normal GJR model. Normal and Student's GJR models are providing very close predictions, while Student's t Realized with leverage generates higher forecasts than those of the same model with Normal distribution. Third panel shows that EGARCH provides higher predictions than Normal GJR model.

D. MSE and MAE for Diebold Mariano test

Table 20: MSE results for Diebold Mariano Test

Table 20 provides the estimated MSE values which are in turn used for comparing out of sample performance of univariate models.

	Coinbase	*Bitfinex*	*Bitstamp*
NGC	1.425E-03	1.226E-03	1.406E-03
TGC	1.416E-03	1.222E-03	1.399E-03
NGS	1.347E-03	1.164E-03	1.329E-03
TGS	2.057E-03	1.594E-03	1.947E-03
NRL	1.935E-03	1.562E-03	1.612E-03
TRL	6.212E-03	2.999E-03	2.685E-03
NGJR	1.525E-03	1.252E-03	1.966E-03
TGJR	1.415E-03	1.229E-03	1.518E-03
NRLL	2.106E-03	1.674E-03	1.684E-03
TRLL	5.159E-03	4.676E-03	2.145E-03
EGC	2.219E-03	1.628E-03	2.217E-03

Table 21: MAE results for Diebold Mariano Test

Table 21 provides the estimate Mean Absolute Error values which are calculated with absolute return as proxy of true volatility. These results can be informative and used to draw conclusions regarding out of sample performance of different models.

	Coinbase	*Bitfinex*	*Bitstamp*
NGC	3.073E-02	2.867E-02	3.057E-02
TGC	3.048E-02	2.858E-02	3.035E-02
NGS	2.934E-02	2.765E-02	2.930E-02
TGS	3.735E-02	3.283E-02	3.626E-02
NRL	3.638E-02	3.251E-02	3.251E-02
TRL	6.959E-02	4.820E-02	4.350E-02
NGJR	3.120E-02	2.892E-02	3.526E-02
TGJR	3.017E-02	2.853E-02	3.137E-02
NRLL	3.814E-02	3.397E-02	3.342E-02
TRLL	6.368E-02	6.158E-02	3.887E-02
EGC	3.973E-02	3.376E-02	3.995E-02

E. Multivariate Plots

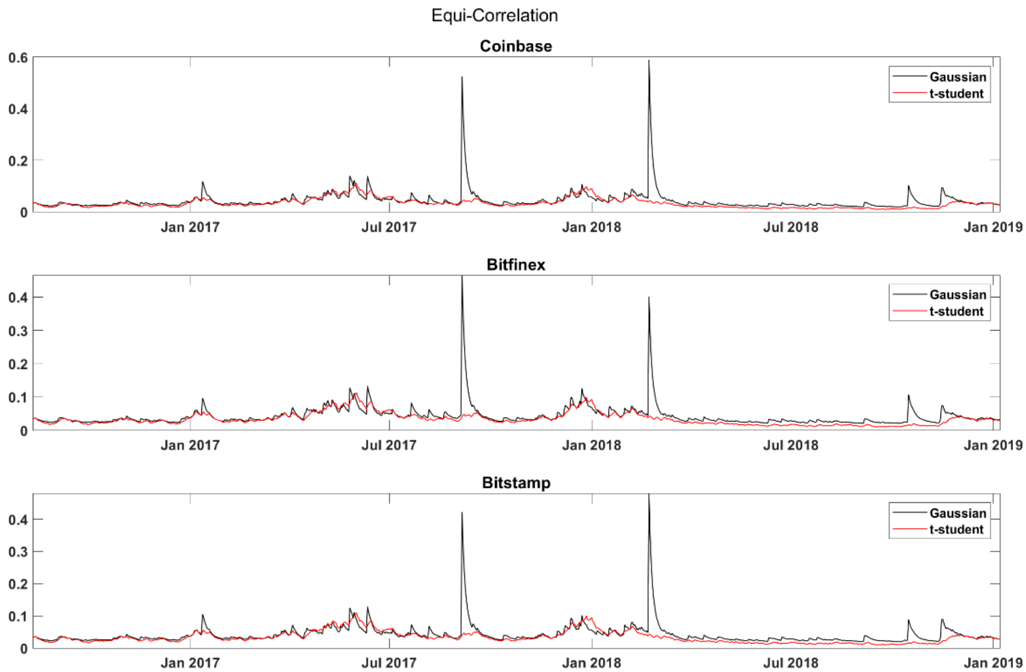

Figure 25: Equi-Correlation Gaussian

Figure 25 depicts forecasted volatilities of all the markets for multivariate GAS with equi-correlation model and Student's t and Normal distributions. This figure shows absorption of outliers and of observations from tails for Student's t distribution.

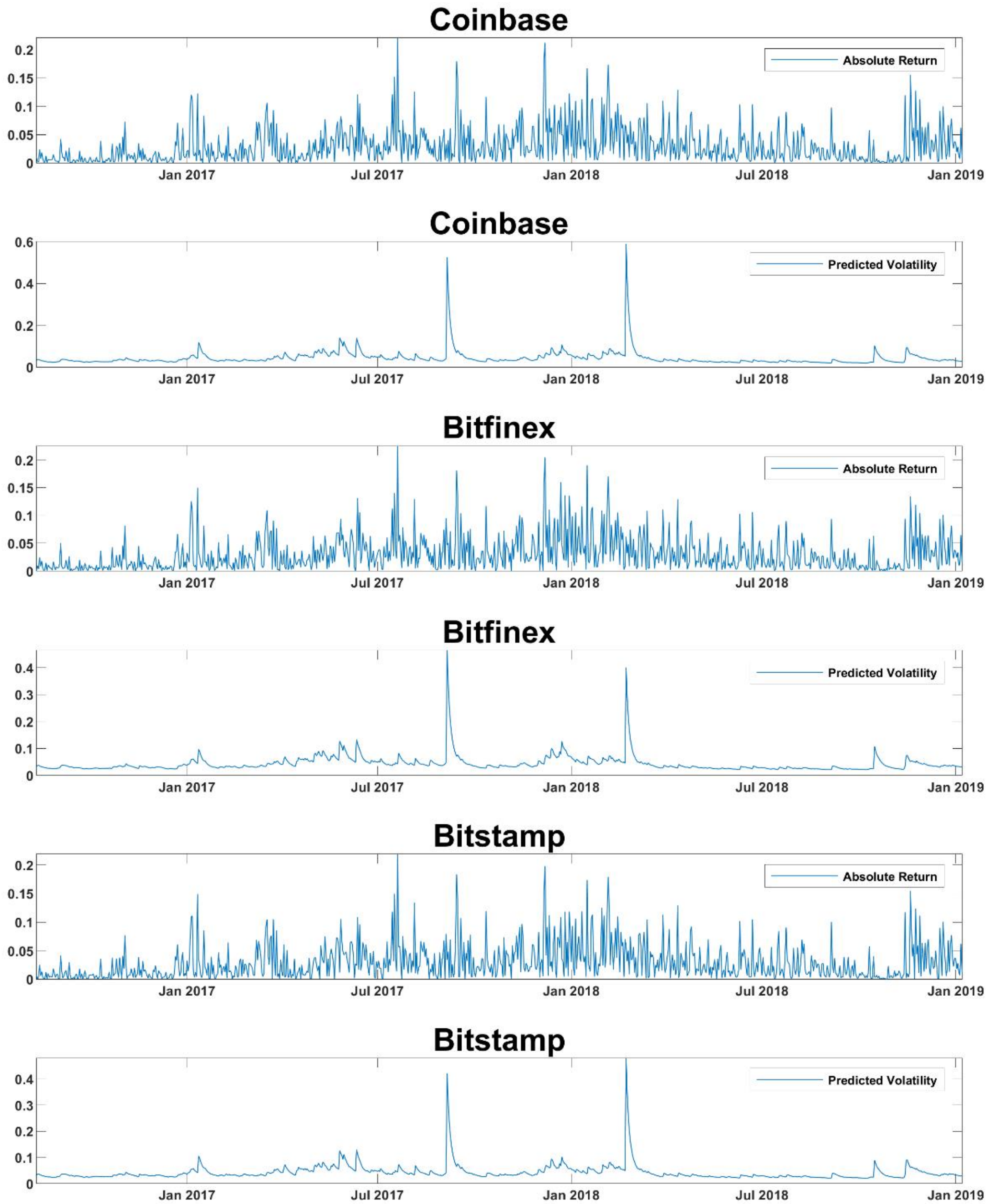

Figure 26: Equi-correlation Gaussian

Figure 26 shows the absolute return and predicted volatility from multivariate GAS model with equi-correlation structure and Normal distribution for all the markets. Two distinct spikes can be seen in prediction for all markets.

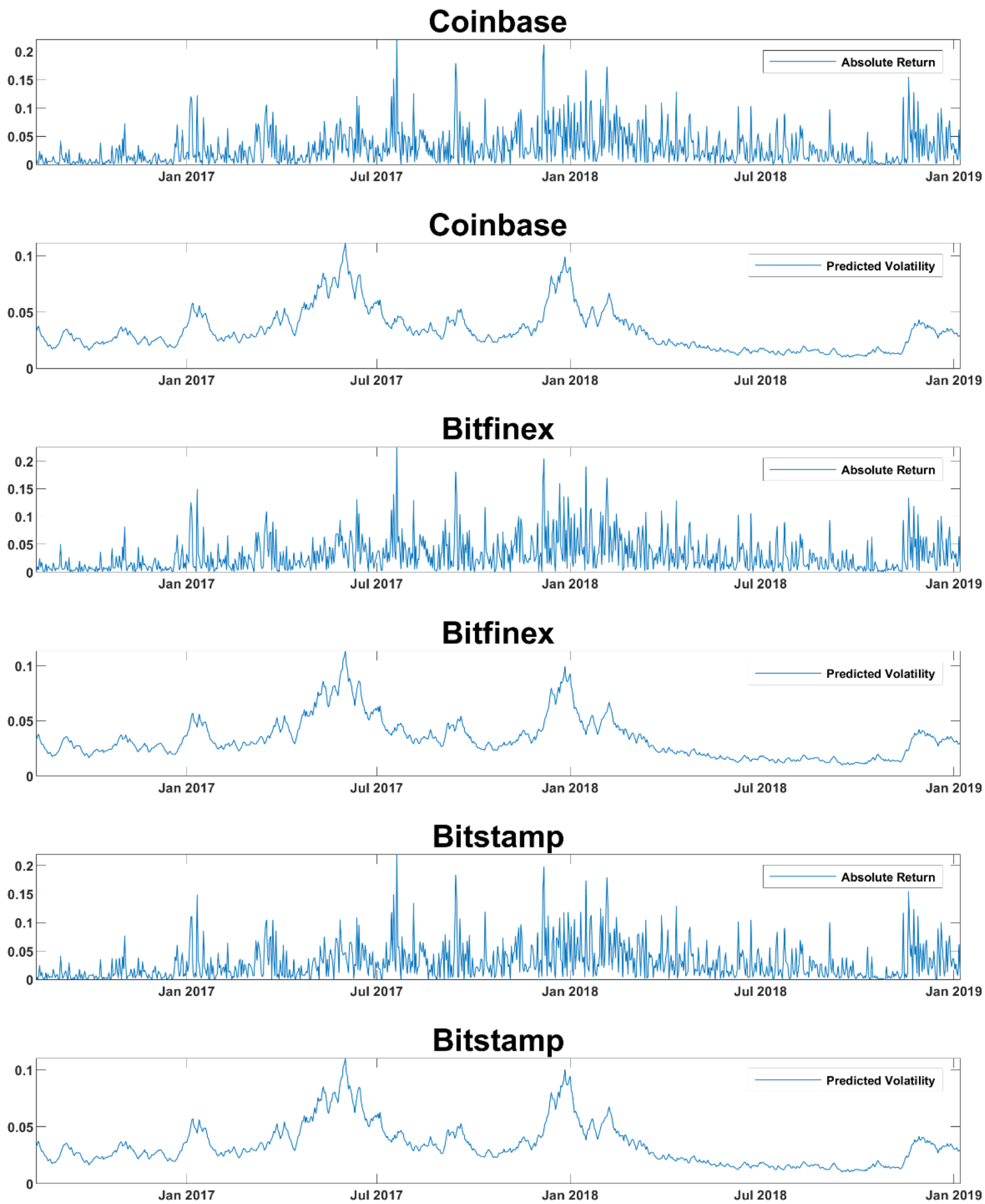

Figure 27: Equi-correlation Student's t

Figure 27 shows the absolute return and predicted volatility from multivariate GAS model with equi-correlation structure and Student's t distribution for all the markets.

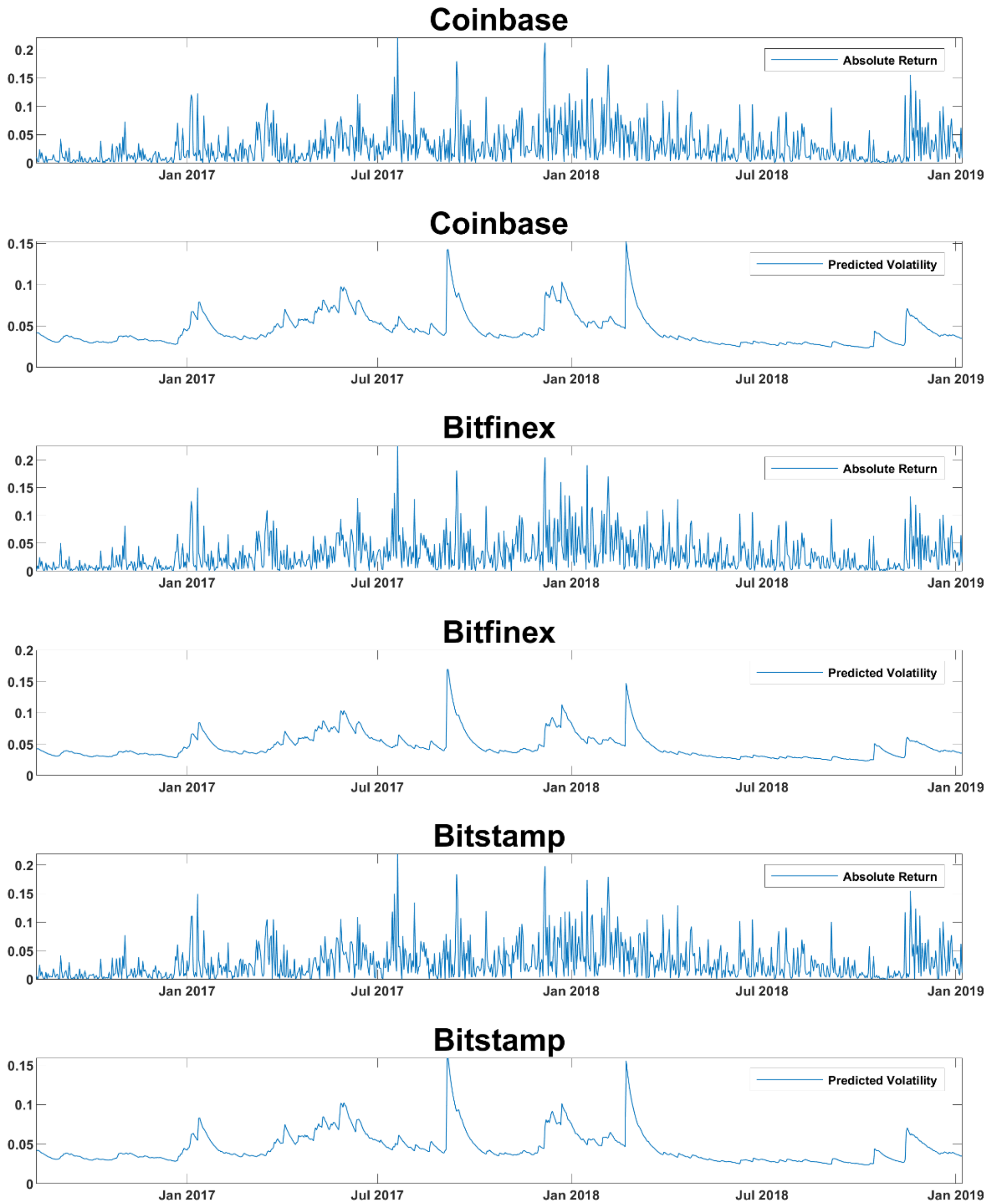

Figure 28: Constant Correlation Gaussian

Figure 28 exhibits the absolute return and predicted volatility from multivariate GAS model with constant correlation structure and Normal distribution for all the markets. Two distinct spikes can be seen in prediction for all markets.

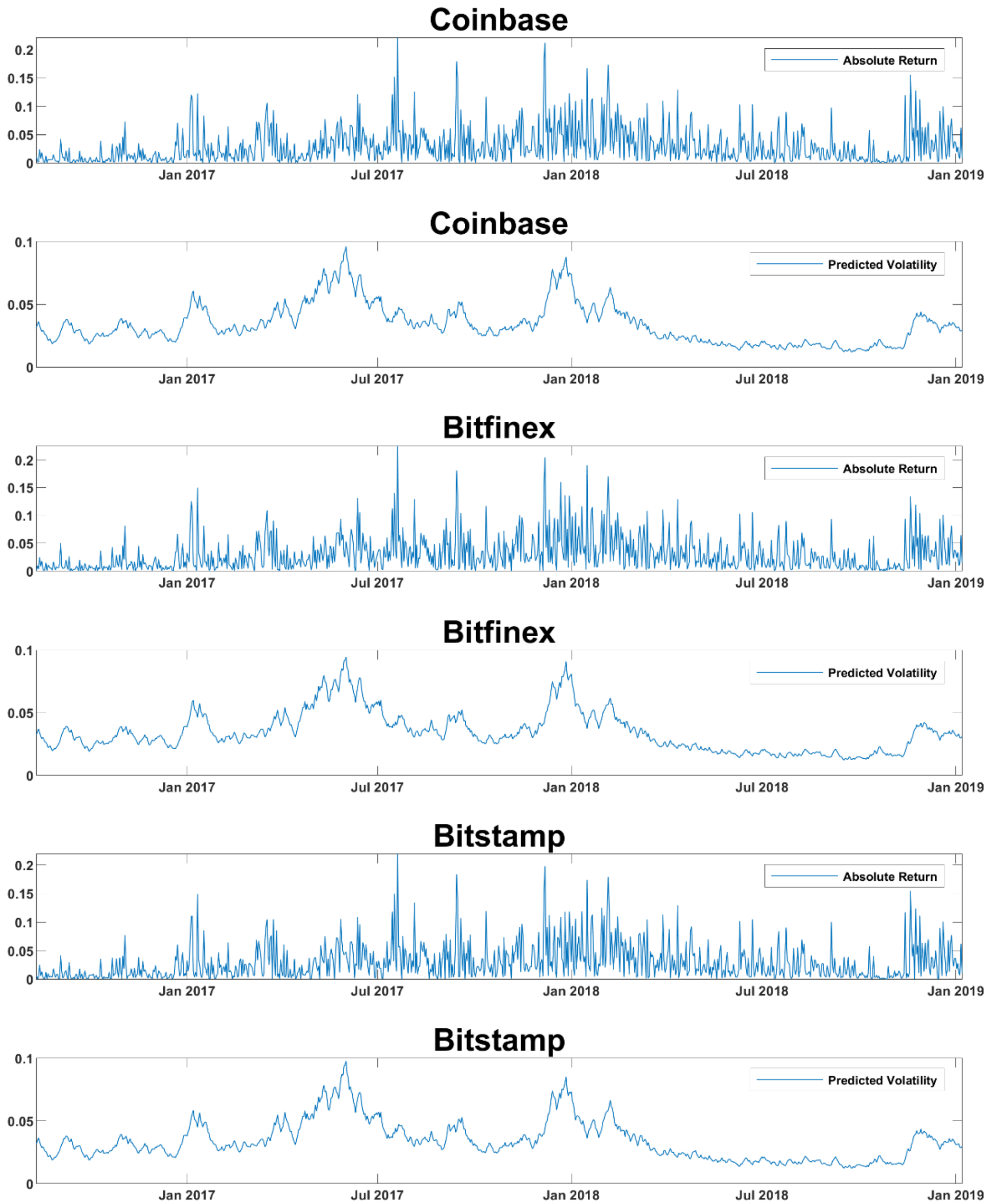

Figure 29: Constant Correlation Student’s t

Figure 29 exhibits the absolute return and predicted volatility from multivariate GAS model with constant correlation structure and Student’s t distribution for all the markets.